Mathematical Biosciences and Engineering

http://www.aimspress.com/journal/MBE

MBE, 19(1): 1–33.
DOI: 10.3934/mbe.2022001
Received: 13 July 2021
Accepted: 18 October 2021
Published: 08 November 2021

Research article

Models to assess imported cases on the rebound of COVID-19 and design a long-term border control strategy in Heilongjiang Province, China

Xianghong Zhang[1], Yunna Song[2,3], Sanyi Tang[4], Haifeng Xue[2], Wanchun Chen[5], Lingling Qin[5], Shoushi Jia[5], Ying Shen[6], Shusen Zhao[6] and Huaiping Zhu[3,*]

[1] Department of Mathematics and Statistics, Southwest University, Chongqing, 400715, China
[2] Basic Medicine School, Qiqihar Medical University, Qiqihar, 161006, China
[3] LAMPS, Department of Mathematics and Statistics, York University, Toronto, ON, M3J 1P3, Canada
[4] School of Mathematics and Information Science, Shaanxi Normal University, Xi'an, 710062, China
[5] Qiqihar Center for Disease Control and Prevention, Qiqihar, 161005, China
[6] Qiqihar Seventh Hospital, Qiqihar, 161006, China

* **Correspondence:** Email: huaiping@mathstat.yorku.ca.

Abstract: Since the outbreak of COVID-19 in Wuhan, China in December 2019, it has spread quickly and become a global pandemic. While the epidemic has been contained well in China due to unprecedented public health interventions, it is still raging or not yet been restrained in some neighboring countries. Chinese government adopted a strict policy of immigration diversion in major entry ports, and it makes Suifenhe port in Heilongjiang Province undertook more importing population. It is essential to understand how imported cases and other key factors of screening affect the epidemic rebound and its mitigation in Heilongjiang Province. Thus we proposed a time switching dynamical system to explore and mimic the disease transmission in three time stages considering importation and control. Cross validation of parameter estimations was carried out to improve the credibility of estimations by fitting the model with eight time series of cumulative numbers simultaneous. Simulation of the dynamics shows that illegal imported cases and imperfect protection in hospitals are the main reasons for the second epidemic wave, the actual border control intensities in the province are relatively effective in early stage. However, a long-term border closure may cause a paradox phenomenon such that it is much harder to restrain the epidemic. Hence it is essential to design an effective border reopening strategy for long-term border control by balancing the limited resources on hotel rooms for quarantine and hospital beds. Our results can be helpful for public health to design border control strategies to suppress COVID-19 transmission.

Keywords: COVID-19; imported cases; time switching system; paradox phenomenon; limited resources; long-term border control

1. Introduction

Heilongjiang Province, located in the northeast of China, shares a 3000-kilometre border with Russia and has 25 border ports. After China took the lead in containing the epidemic, the province had become one of the main regions in the world to be suffering the second outbreak because of a large inflow of people from abroad [1]. No new or suspected infected cases had been reported in Heilongjiang Province, China since March 10, 2020, and all confirmed cases were cured on March 26, 2020. However, there were 69 confirmed local cases in the province from April 11 to April 27, 2020, accounting for 68 percent of the country's total cases [2].

The main reason for the second outbreak in Heilongjiang Province may be the surge in the number of people imported from abroad. Suifenhe is a border town of just 70,000 people in Heilongjiang Province, China. Taking Suifenhe border port in the province as an example, an average of 178 people entered the city every day from March 26 to April 4, and the number reached a peak value 495 on April 4, 2020 [2]. It is far beyond the prevention and control capacity of Suifenhe town. In addition, with increasing severity of epidemic in foreign countries, General Administration of Civil Aviation of China (CAAC) implemented the 'five ones' flight policy. It means that each domestic airline company can only reserve one route to each country, and that each route can not operate more than one flight each week, so do foreign airlines [3, 4]. Meanwhile, the Chinese government adopted the diversion policy on some major entry ports, except for Suifenhe port [5], which also brought great pressure on epidemic prevention and control in the province.

Therefore, Chinese and Russian governments have decided to temporarily close Suifenhe port to suppress the spread of epidemic since April 7, 2020 [6]. At the same time, some sections of Suifenhe town were under traffic control in April 9 [7], then all communities were closed in April 11 [8] and other related control policies were carried out in time [9]. On April 2, the epidemic prevention and control headquarters of Heilongjiang Province issued the 14th announcement: strictly implementing six measures of 100% and 'closed-loop' control [10].

However, there is still the epidemic risk from imported cases due to the complicated terrain, frequent trade between China and Russia. Moreover, compared with the epidemic in China having been effectively restrained, the fear to the severity of epidemic in Russia will make more people seek for a safer region by entering China through Suifenhe port, and may increase the number of infected importing people. At present, the border port has been closed about 10 months and maybe longer. The long-term border closure in the port will further cause more people to decide illegal importing via taking risks. And illegal imported cases may greatly increase the potential spreading risk of the epidemic since they are much harder to be monitored in time. Therefore, a long-term border closure may cause a paradox phenomenon in epidemic control. It indicates that it may be more difficult to block the epidemic for a long-term border closure than that for a border reopening, which may cause new epidemic rebounds in Heilongjiang Province. The features of the epidemic outbreaks in the province are sporadic in many regions. For example, a new epidemic appeared in Dongning City on December 10, 2020, a national first-level border ports in Heilongjiang Province [11]. On January 20, 2021, a total of 68 cases were confirmed in a single day, and 85 new asymptomatic infected cases were reported in the province [12].

Many dynamic models were proposed to study the spread of COVID-19 with imported cases, and

their results are useful to understand the impact of imported cases on epidemic outbreaks or design effective border closure strategies in a short-term duration [13–31]. At present, there are more than 100 million confirmed cases worldwide, so we should investigate how to fight against imported novel coronavirus for a future long-term duration. Moreover, it is necessary to explore whether the epidemic rebounds are caused by the long-term border closure? If so, it is urgent to design a plan for reopening the border in the province. Given the extensive border and numerous border ports in Heilongjiang Province, it is essential to study the management of imported cases and control of COVID-19 epidemic in the province.

In this paper, we extend the classical SEAIR compartmental framework to build a time switching dynamical system to depict the transmission process of COVID-19 in three stages in Heilongjiang Province, China. The model will combine with epidemic prevention and control strategies in the province, including the government interventions (such as contact tracing and quarantine of both local and importing populations, testing and diagnosing on infected cases, border closure), individual compliance intensities (such as contract rate, the number of importing populations, the protection intensity on nosocomial infection). Cross validation of parameter estimations was carried out by fitting the model with eight time series of cumulative numbers in the province simultaneously to improve its credibility. Then we found that illegal imported cases and imperfect protection intensity of nosocomial infection are the main reasons for the second epidemic wave, and the actual border control intensities are relatively effective in early control stage. Simulations showed the existence of a paradox phenomenon under a long-term border closure. Hence combination with reducing economic losses, people's psychological burden, we define the daily reasonable number of legal importing population by considering the resource limitations of hotel rooms and hospital beds. On this basis, the reopening measure of border ports is designed for a long-term border control, which could inform public health decision-makers carrying out the best border reopening strategy. Our results will not only help to contain the spread of the epidemic in the province, but also can be referred for epidemic control in other regions.

2. Method

2.1. Data

From the Health Commission of Heilongjiang Province, China, we noticed that there were no new confirmed cases, no new suspected cases, no new confirmed importing cases from abroad, all 482 confirmed cases have been cured expect for 13 death cases, and all 16,389 close contacts have been released from medical observation on March 26, 2020 in the province. And there is a similar situation on July 1, 2020, but all 465 confirmed cases have been cured, and 4153 out of 4157 close contacts have been released from medical observation. Thus the duration of the second wave of COVID-19 epidemic in the province are approximately from March 26 to July 1, 2020. In this work, the eight time series of cumulative numbers related with COVID-19 in the duration are chosen as shown in Figure 1. It should be mentioned that the cumulative number of local quarantined cases contains the cumulative numbers of susceptible cases in quarantine together with exposed or infected cases in isolation.

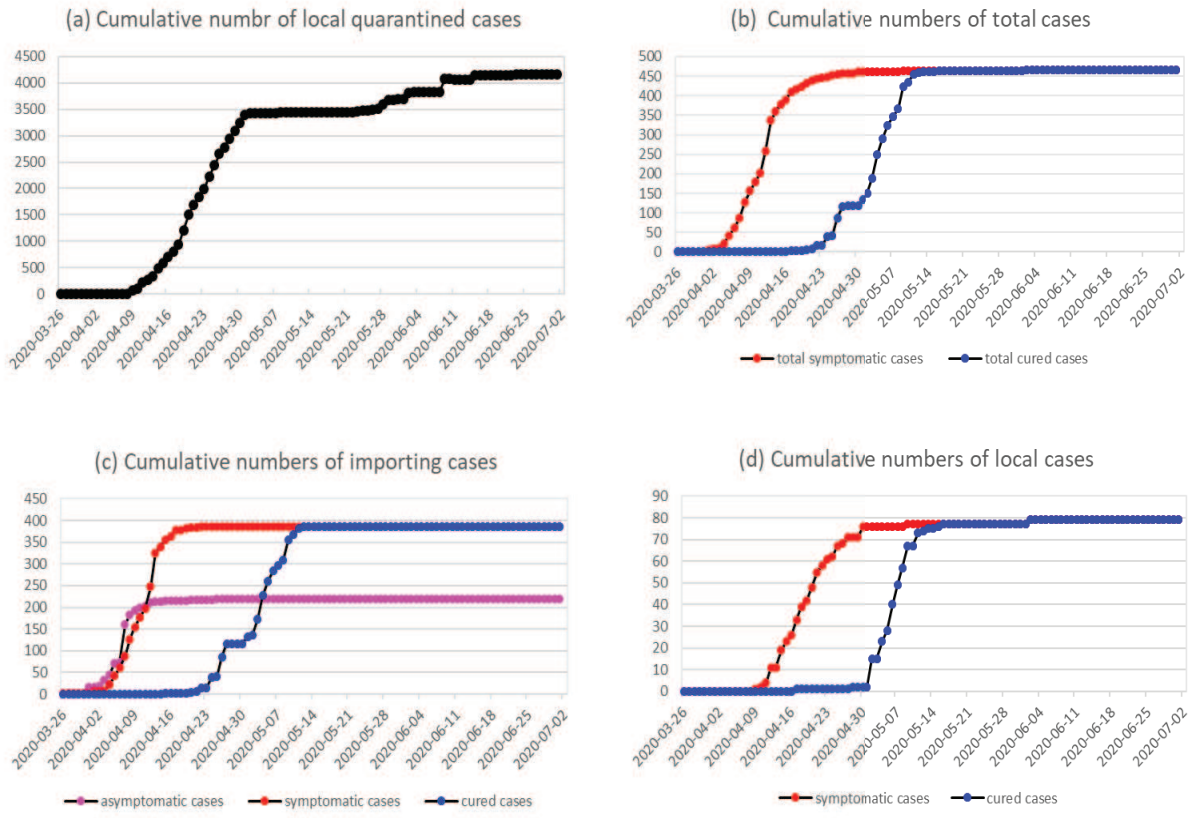

Figure 1. The eight data series related with COVID-19 in Heilongjiang Province, China from March 26 to July 1, 2020. (a) Cumulative number of local quarantined cases (black), (b) cumulative numbers of local and importing symptomatic (red) and cured (blue) cases, (c) cumulative numbers of importing asymptomatic (magenta), symptomatic (red) and cured (blue) cases, (d) cumulative numbers of local symptomatic (red) and cured (blue) cases.

2.2. Model overview

The Chinese government has imposed strictly centralized quarantine on legal returnees upon entry since March 21, 2020, while there is no quarantine strategy for illegal returnees. Compared with the strict movement restriction for local population under supervision, local population escaping from supervision can move freely within the province to some extent. It indicates that there are different population routes and intervention strategies for legal and illegal importing populations and for local populations under supervision and without supervision. Hence the importing population is divided into legal and illegal ones, while the local population is separated as freedom and control parts. We will investigate the effects of importing cases and control strategies on the rebound of COVID-19 endemic in Heilongjiang Province.

Local population with freedom. Note that the incubation period accounts for a relative long duration of the whole disease transmission period, and the exposed individuals in the late incubation period can transmit the virus into other susceptible individuals. There is a large proportion of asymptomatic infectious individuals. We extend the transmission model Susceptible-Exposed in the first stage (non-infectious)-Exposed in the second stage (infectious)-Infectious without symptoms-Infectious with symptoms-Recover framework, by introducing variables S, E_1, E_2, A, I and R, respectively.

Legal importing population. Denote the daily number of legal importing population during border opening as $V_q(t)$. All the legal returnees upon entering the border are compulsively quarantined into the nearby separated hotel rooms in the province, denoted as Q_F compartment. Note that all quarantined individuals in the hotel rooms are forced to undergo multiple nucleic acid tests. According to the first testing result, the legal importing population will be arranged into corresponding cabins. To be exact, positive individuals without symptoms will be regarded as asymptomatic infected ones and to be observed in hospitals (W_F), positive individuals with symptoms will be diagnosed as confirmed cases to be treated in hospitals (H_F). If individuals' testing results are negative within 14-day quarantine period, then they will continue stay in Q_F, or until the end of quarantine period they will be released into S. Similarly, for the second and subsequent nucleic acid tests, legal importing individuals will be moved into the corresponding cabins (W_F or H_F) once their testing results become positive during the quarantine period.

Illegal importing population. Some individuals may want to timely come across the border without quarantine by choosing illegal importing way. Denote the daily number of illegal importing population during border opening as $V_p(t)$. Note that there is no intervention strategy for illegal importing population. It will be at any epidemic phases for illegal importing population entering the border and mixing together with local population. Denote the proportions of illegal importing population being the five epidemic phases as $\theta_S, \theta_{E1}, \theta_{E2}, \theta_A, \theta_I$, respectively.

Local population under control. Note that close tracking quarantine and testing strategy are strictly implemented in the province. Local susceptible population closely contacting with infected ones may be infected ($qc\beta S\Pi/N$) or not be infected ($qc(1-\beta)S\Pi/N$), who will then be tracked and quarantined into local quarantine compartments Q_D or Q_S, respectively. A proportion of exposed in the second stage individuals (E_2) and infectious without symptoms individuals (A) will be moved into medicine observation wards (W_D). And a proportion of infectious with symptoms individuals (I) will be diagnosed as confirmed cases and moved into medicine treatment wards (H_D).

To explore the effect of importing population on the transmission of COVID-19 during different

control stages, here we introduce three time intervals (here $T_0 \le t < T_1, T_1 \le t < T_2, t \ge T_2$) as the three phases I, II and III, respectively. Time points T_0, T_1 and T_2 are the initial time (March 26th 2020), the actual switching time from border opening to one border closure intensity (April 7th 2020) and the further possible switching time from the border closure intensity to another closure intensity, respectively.

Actually, border closure strategy may change the behavior of individuals originally intend to enter the border legally or illegally. A proportion of individuals intend to enter legally will choose to enter illegally during border closure. And the number of legal and illegal importing individuals during phases II and III may decrease by certain percentages, denoted by α_i and $\hat{\alpha}_i (i = p, q)$, respectively. Especially, a long-term border closure can cause more people to choose illegal importing by taking a risk, so we assume that the maximum number of importing population in phase III will be increased to f_q and f_p times that in the first two phases, respectively. Then we define the legal and illegal importing populations in the three stages as follows

$$V_q(t) = \begin{cases} (V_{q0} - V_{qb})e^{-r_q t} + V_{qb}, & if\ T_0 \le t < T_1, \\ (1-\alpha_q)((V_q(T_1) - V_{qb})e^{-r_q(t-T_1)} + V_{qb}), if\ T_1 \le t < T_2, \\ (1-\hat{\alpha}_q)((V_q(T_2) - f_q V_{qb})e^{-r_q(t-T_2)} + f_q V_{qb}), if\ t \ge T_2, \end{cases}$$

and

$$V_p(t) = \begin{cases} (V_{p0} - V_{pb})e^{-r_p t} + V_{pb}, & if\ T_0 \le t < T_1, \\ (1-\alpha_p)((V_p(T_1) - V_{pb})e^{-r_p(t-T_1)} + V_{pb}), if\ T_1 \le t < T_2, \\ (1-\hat{\alpha}_p)((V_p(T_2) - f_p V_{pb})e^{-r_p(t-T_2)} + f_p V_{pb}), if\ t \ge T_2. \end{cases}$$

Moreover, we assume that the percentages of illegal importing population for each infection state are the same during the first two sages for simplicity. To investigate the severity of the epidemic in neighboring countries on the disease rebound in the province, we assume that the percentages of illegal importing population being infected ones increase to $f_\theta \theta_{j0} (j = E_1, E_2, A, I)$ in phase III. Then we define

$$\theta_j = \begin{cases} \theta_{j0}, & if\ T_0 \le t < T_2, \\ f_\theta \theta_{j0}, if\ t \ge T_2, \end{cases} \quad j = E_1, E_2, A, I,$$

and

$$\theta_S = \begin{cases} \theta_{S0}, & if\ T_0 \le t < T_2, \\ 1 - f_\theta(\theta_{E10} + \theta_{E20} + \theta_{A0} + \theta_{I0}), if\ t \ge T_2. \end{cases}$$

In addition, we define

$$\varepsilon = \begin{cases} 0, if\ T_0 \le t < T_1, \\ 1, if\ t \ge T_1, \end{cases}$$

where ε being equal to 0 and 1 are used to depict the border opening and closure, respectively.

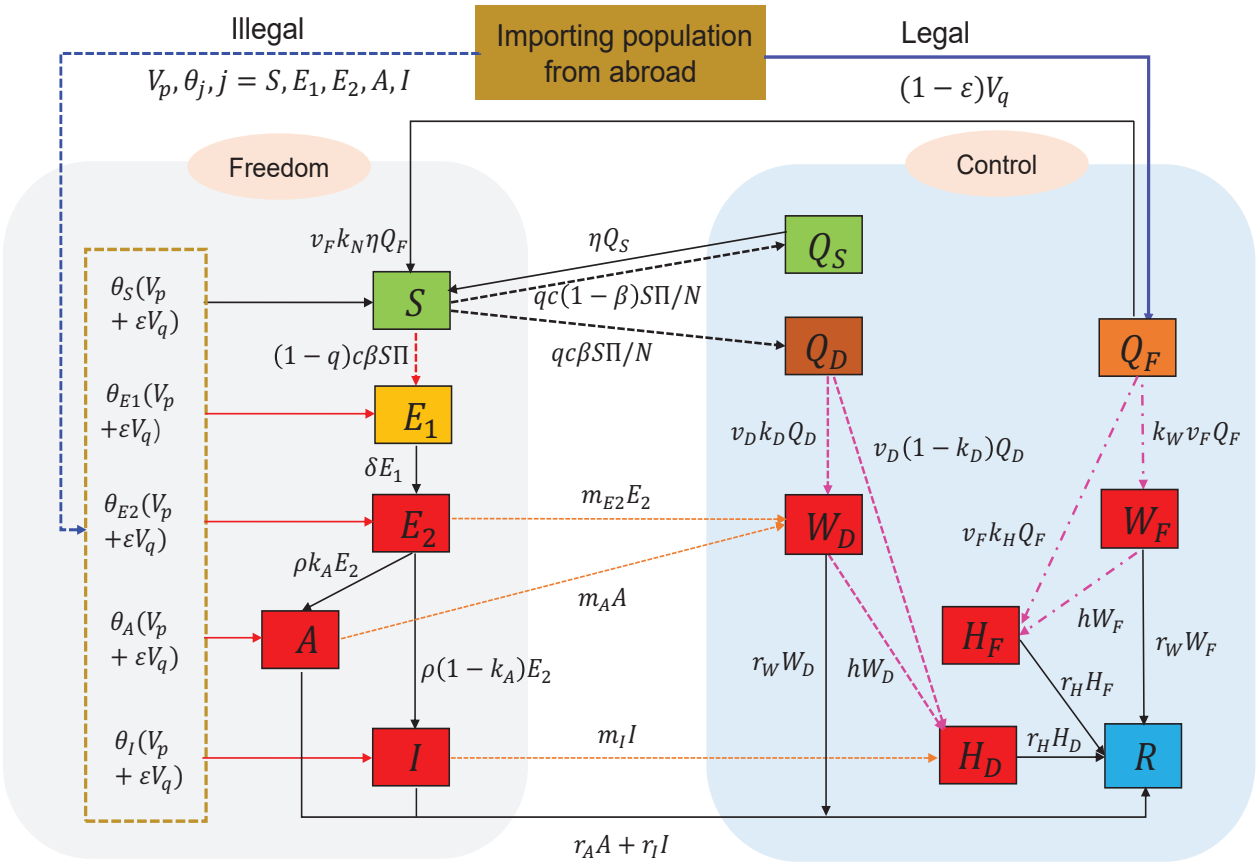

Figure 2. A flow diagram of model (2.1) adopted in this study for illustrating the imported cases on the second outbreak of COVID-19 epidemic in Heilongjiang Province, China. Solid and dashed blue lines are the legal and illegal importing routes, respectively. The freedom and control plates means the corresponding populations being out of supervised and supervised, respectively. Variable ε being equal to 0 or 1 indicates the border port is opened or closed, respectively. Solid red and black lines are population progression routes. Red, black and brown dashed lines are disease transmission routes, the quarantining routes for intensive contact tracing and the testing routes of freedom infectious individuals, respectively. Magenta dashed (or dot-dashed) lines are the transfer routes among local (or importing) quarantined individuals and infected ones in hospitals.

Based on above assumptions and the flow diagram in Figure 2, we build the model as follows

$$\begin{cases} S^{'} = \theta_S \left(V_p(t) + \varepsilon V_q(t)\right) - \frac{((1-q)\beta+q)cS\Pi}{N} + k_N v_F \eta Q_F + \eta Q_S, \\ E_1^{'} = \theta_{E1} \left(V_p(t) + \varepsilon V_q(t)\right) + \frac{(1-q)\beta cS\Pi}{N} - \delta E_1, \\ E_2^{'} = \theta_{E2} \left(V_p(t) + \varepsilon V_q(t)\right) + \delta E_1 - \rho E_2 - m_{E2} E_2, \\ A^{'} = \theta_A \left(V_p(t) + \varepsilon V_q(t)\right) + k_A \rho E_2 - r_A A - m_A A, \\ I^{'} = \theta_I \left(V_p(t) + \varepsilon V_q(t)\right) + (1-k_A)\rho E_2 - r_I I - m_I I, \\ Q_F^{'} = (1-\varepsilon)V_q(t) - (k_W + k_H + k_N \eta) v_F Q_F, \\ Q_D^{'} = \frac{qc\beta S\Pi}{N} - v_D Q_D, \\ Q_S^{'} = \frac{qc(1-\beta)S\Pi}{N} - \eta Q_S, \\ W_F^{'} = k_W v_F Q_F - r_W W_F - h W_F, \\ W_D^{'} = k_D v_D Q_D + m_{E2} E_2 + m_A A - r_W W_D - h W_D, \\ H_F^{'} = k_H v_F Q_F + h W_F - r_H H_F, \\ H_D^{'} = (1-k_D) v_D Q_D + h W_D + m_I I - r_H H_D, \\ R^{'} = r_A A + r_I I + r_W (W_F + W_D) + r_H (H_F + H_D), \end{cases} \tag{2.1}$$

with $N = S + E_1 + E_2 + A + I + Q_F + Q_D + Q_S + W_F + W_D + H_F + H_D + R$ and $\Pi = I + u_1 A + u_2 E_2 + u_3(W_F + W_D) + u_4(H_F + H_D)$. In fact, the item Π indicates all possible infection sources of the disease. The items $(1-\varepsilon)V_q$ and $V_p + \varepsilon V_q$ are the actual daily number of legal and illegal importing population, respectively. The detailed description of all variables and parameters in Figure 2 and model (2.1) are shown in Tables 1, 2 and 3.

Table 1. Descriptions, initial values and sources of state variables for model (2.1).

Variable	Description	Initial value[(95% CI), Std]	Source
S	No. of susceptible individuals	18854[(1.8845,1.8863)e4, 626.83]	Estimated
E_1	No. of non-infectious exposed individuals	0	Assumed
E_2	No. of infectious exposed individuals	0	Assumed
A	No. of asymptomatic infectious individuals	0	Assumed
I	No. of symptomatic infectious individuals	0	Assumed
Q_F	No. of importing quarantined individuals	203	Data
Q_D	No. of local quarantined individuals being infected	0	Data
Q_S	No. of local quarantined individuals being susceptible	0	Data
W_F	No. of importing asymptomatic infectious individuals in hospitals	0	Data
W_D	No. of local asymptomatic infectious individuals in hospitals	0	Data
H_F	No. of importing symptomatic infectious individuals in hospitals	2	Data
H_D	No. of local symptomatic infectious individuals in hospitals	0	Data
R	No. of recovered individuals	0	Data

Table 2. General parameter descriptions, values(Std), 95% CI and sources for models (2.1).

Para.	Description	Value(Std)	95% CI	Unit	Source
c	Contact rate	5.1315(2.1453e-1)	(5.1286,5.1346)	$p^{-1}day^{-1}$	Estimated
β	Probability of transmission per contact	0.0024992(9.6232e-05)	(2.4978,2.5005)e-3	$p^{-1}day^{-1}$	Estimated
u_1	Adjustment factor of contact rate with asymptomatic infectious individuals	0.89511(8.6459e-2)	(8.9389,8.9629)e-1	N/A	Estimated
u_2	Adjustment factor of contact rate with infectious exposed individuals	0.60683(1.4720e-2)	(6.0662,6.0702)e-1	N/A	Estimated
u_3	Adjustment factor of contact rate with asymptomatic infectious individuals in hospitals	1.1521(4.7558e-2)	(1.1515,1.1528)	N/A	Estimated
u_4	Adjustment factor of contact rate with symptomatic infectious individuals in hospitals	1.1339(2.8536e-2)	(1.1335,1.1343)	N/A	Estimated
δ	Transition rate from non-infectious exposed individuals to the infectious exposed ones	1/5(/)	/	day^{-1}	[37]
ρ	Transition rate from infectious exposed individuals to the infectious ones	1/3(/)	/	day^{-1}	[37]
η	Releasing rate of the quarantined uninfected individuals into the wider community	1/14(/)	/	day^{-1}	[33]
r_A	Natural recovery rate of asymptomatic infectious individuals	0.1497(/)	/	day^{-1}	[35]
r_I	Natural recovery rate of symptomatic infectious individuals	0.1029(/)	/	day^{-1}	[35]
r_W	Recovery rate of asymptomatic infectious individuals in hospitals	0.069457(5.3092e-4)	(6.9450,6.9465)e-2	day^{-1}	Estimated
r_H	Recovery rate of symptomatic infectious individuals in hospitals	0.081665(9.4146e-4)	(8.1651,8.1677)e-2	day^{-1}	Estimated
q	Quarantined rate of exposed individuals	0.10366(3.0272e-3)	(1.0362,1.0370)e-1	day^{-1}	Estimated
v_F	Test rate of importing quarantined individuals	1/2	/	day^{-1}	Data
v_D	Test rate of local quarantined individuals	0.280244(2.9656e-3)	(2.8020,2.8028)e-1	day^{-1}	Estimated
k_A	Transition probability of asymptomatic infectious individuals from exposed ones	0.6(/)	/	day^{-1}	[34]
k_W	Percentage of quarantined importing individuals being asymptomatic infected	0.024348(4.3612e-4)	(2.4342,2.4354)e-2	N/A	Estimated
k_H	Percentage of importing quarantined individuals being confirmed cases	0.018201(4.7973e-4)	(1.8194,1.8207)e-2	N/A	Estimated
k_N	Percentage of quarantined importing individuals being susceptible	0.957451(/)	/	N/A	$1-k_W-k_H$
k_D	Percentage of local quarantined individuals being asymptomatic infected	0.85281(3.5164e-2)	(8.5232,8.5330)e-1	N/A	Estimated
m_{E2}	Diagnose rate of exposed infectious individuals	0.18111(1.2844e-2)	(1.8093,1.8129)e-1	day^{-1}	Estimated
m_A	Diagnose rate of asymptomatic infectious individuals	0.18688(6.2376e-3)	(1.8679,1.8696)e-1	day^{-1}	Estimated
m_I	Diagnose rate of symptomatic infectious individuals	0.37121(1.9502e-2)	(3.7094,3.7149)e-1	day^{-1}	Estimated
h	Transition rate from asymptomatic infectious individuals in hospitals to confirmed cases	0.20811(1.7137e-3)	(2.0809,2.0814)e-1	day^{-1}	Estimated

p: person.

Table 3. Importing related parameter descriptions, values(Std), 95% CI and sources for models (2.1).

Para.	Description	Value(Std)	95% CI	Unit	Source
θ_S	Percentage of illegal importing individuals being susceptible	0.8224(2.8054e-1)	(8.2163,0.8.2240)e-1	N/A	Estimated
θ_{E1}	Percentage of illegal importing individuals being non-infectious exposed	0.0396(1.7152e-2)	(3.9548,3.9595)e-2	N/A	Estimated
θ_{E2}	Percentage of illegal importing individuals being infectious exposed	0.0360(2.5274e-2)	(3.5931,3.6000)e-2	N/A	Estimated
θ_A	Percentage of illegal importing individuals being asymptomatic infectious	0.0252(2.2437e-2)	(2.5174,0.02.5236)e-2	N/A	Estimated
θ_I	Percentage of illegal importing individuals being symptomatic infectious	0.0768(1.9134e-2)	(7.6722,7.6775)e-2	N/A	Estimated
V_{p0}	Introducing rate of illegal importing individuals at the initial time	5.9726(3.4430e-1)	(5.9679,5.9775)	day^{-1}	Estimated
V_{q0}	Introducing rate of legal importing individuals at the initial time	20.371(9.4832e-1)	(2.0358,2.0384)	day^{-1}	Estimated
V_{pb}	Maximum introducing rate of illegal importing individuals under the policy	20.181(1.8905e-1)	(2.0178,2.0184)		Estimated
V_{qb}	Maximum introducing rate of legal importing individuals under the policy	57.496(2.0989)	(5.7468,5.7526)	day^{-1}	Estimated
r_1	Exponential increasing rate of introducing rate for illegal importing	0.043606(9.7476e-4)	(4.3592,4.3619)e-2	N/A	Estimated
r_2	Exponential increasing rate of introducing rate for legal importing	0.074462(9.4035e-4)	(7.4450,7.4475)e-2	N/A	Estimated

Para.	Description	Value range	Unit	Source
α_i	Compliance rate of individuals on border closure in phase II, $i = p, q$ for illegal or legal situation	[0, 1]	N/A	Assumed
$\hat{\alpha}_i$	Compliance rate of individuals on border closure in phase III, $i = p, q$ for illegal or legal situation	[0, 1]	N/A	Assumed
f_i	Adjustment factor on the maximum number of importing individuals in phase III, $i = p, q$	related to the epidemic	N/A	Assumed
f_θ	Adjustment factor on the proportion of illegal importing individuals in phase III	related to the epidemic	N/A	Assumed

Next, model (2.1) will used to reflect the effects of legal and illegal importing populations on the transmission of the disease in Heilongjiang Province, China. We will first fitting the model to the eight data categories and assess the transmission risk of the disease. Then we will investigate the possible reasons for the second outbreak of the disease, and assess the effectiveness of early border strategies. Especially, we explore a potential paradox or risk for long-term border closure if there are still serious epidemics in some neighbour countries. Thus to avoid the potential risk, we finally explore the border reopening measure under limiting resources for disease control.

3. Results

3.1. Risk assessment

The basic reproduction number R_0 means the average number of individuals infected by the introduction of a single infected one in the whole susceptible population. According our data collection of the province, there is no new dead case from COVID-19 during the second outbreak. Thus under the assumptions of no importing population and ignoring disease-induced death rate, there exists a disease-free equilibrium for the model. Then we first calculate the effective reproduction number R_t by using the next generation matrix method [32], as shown in Appendix A. From Eq (S4) in Appendix A, the formula of R_t is a function with respect to time t, and it exists the term $S(t)/N(t)$. Next if let $t = 0$, then we can directly obtain the formula of R_0. Note that in the beginning of the disease rebound, it is reasonable to assume that the initial number of susceptible population (*i.e.*, $S(0)$) would approximate to the number of total populations (*i.e.*, $N(0)$), then the term $S(0)/(N(0)$ can be simplified as one. By removing the term $S(t)/N(t)$ in Eq. (S4), we can obtain the formula of R_0 as

$$R_0 = R_{01} + R_{02} + R_{03} + R_{04} + R_{05}. \tag{3.1}$$

It should be mentioned that $R_{01}, R_{02}, R_{03}, R_{04}$ and R_{05} indicate the average number of individuals infected by the introduction of a single infected individual of I, A, E_2, W_F or W_D and H_F or H_D in the whole susceptible population, respectively. The detailed calculation process are shown in Appendix A.

3.2. Parameters

All parameters in model (2.1) can be divided into deterministic and estimated ones. We firstly fix the deterministic parameters and the initial values from official survey reports, previous literatures and the data information to reduce the complexity as show in Tables 1 and 2. The latent periods in E_1 and E_2 stages are fixed as 5 and 3 days, respectively, i.e., $\delta = 1/5$ and $\rho = 1/3$ [37]. The testing rate of quarantined legal importing individuals and the releasing rate of uninfected individuals under quarantine are fixed as $v_F = 1/2$ and $\eta = 1/14$, respectively [33]. Notice that there is a quick response to the second wave of COVID-19 epidemic in Heilongjiang Province and timely medical supplies from other provinces, and there is no death cases from March 26 to July 1, 2020, so we ignore the disease induced death rate in hospitals. The recovery rates of asymptomatic and symptomatic infectious individuals are fixed as $r_A = 0.1497$ and $r_I = 0.1029$, respectively [35]. And the transition probability from E_2 to A is fixed as $k_A = 0.6$ [34]. According to the data information, we fix the initial values of Q_F and W_F as 203 and 2, respectively. Since on March 26, 2020, there is no newly confirmed symptomatic and asymptomatic cases, all local confirmed or quarantined cases are cured or

removed from close medical observation, respectively, so we reset initial cumulative numbers of local quarantined, reported symptomatic and cured cases and other initial components being zero.

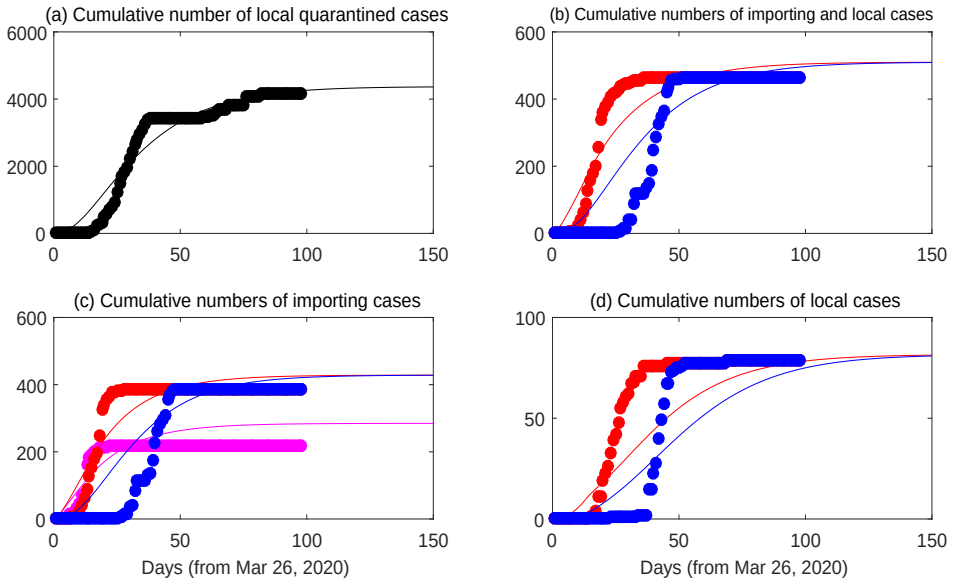

Figure 3. Goodness fitting results and validations of model (2.1) with the eight cumulative data categories from March 26 to July 1, 2020 and from July 2 to Aug 22, 2020 for Heilongjiang Province, China. The color curves or circles are the goodness fitting results or the corresponding cumulative data, respectively. The cumulative data used in (a), (b), (c) and (d) are the same as the ones in Figure 1(a), (b), (c) and (d), respectively.

To estimate the values, standard deviations (Std) and 95% CI of the index parameters and initial value of susceptible individuals (see Tables 1, 2 and 3), we simultaneously fit the proposed model (2.1) to the eight cumulative data categories from March 26 to July 1, 2020 (see Figure 1) by carrying out the Markov Chain Monte Carlo (MCMC) procedure [36]. In Figures 3 and 4, the best fitting results are marked as color curves. The same color circles represent the corresponding data from March 26 to July 1, 2020, while the color curves between July 2 to Aug 22, 2020 are used to verify our estimation and predict the trends of solution curves. Specifically, the black, magenta, red and blue solid circles (or curves) represent the cumulative number of local quarantined individuals, reported asymptomatic, reported symptomatic and cured cases (or the best fitting results), respectively. Moreover, the best fitting results and their 95% CI curves are shown in Figure 4. The yellow and cyan curves denote the 95% upper and lower confidence limits. In addition, the trends of the eight cumulative data are flat due to almost no change on those data between July 2 to Aug 22, 2020, so we do not show them in the figures.

It is worth mentioning that the eight time series of data are used to fit the model simultaneously, which can help to cross-validating the estimation results and improve their credibility. It is difficult to fit well the model with the eight time series of data simultaneously in a long time interval. From Figures 3 and 4, although our fitting results are a little higher than their real data during the steady states since some strong interventions are carried out after April 7. However, the fitting results are well during the initial stage of the second outbreak. Moreover, we assume a priori distribution for each

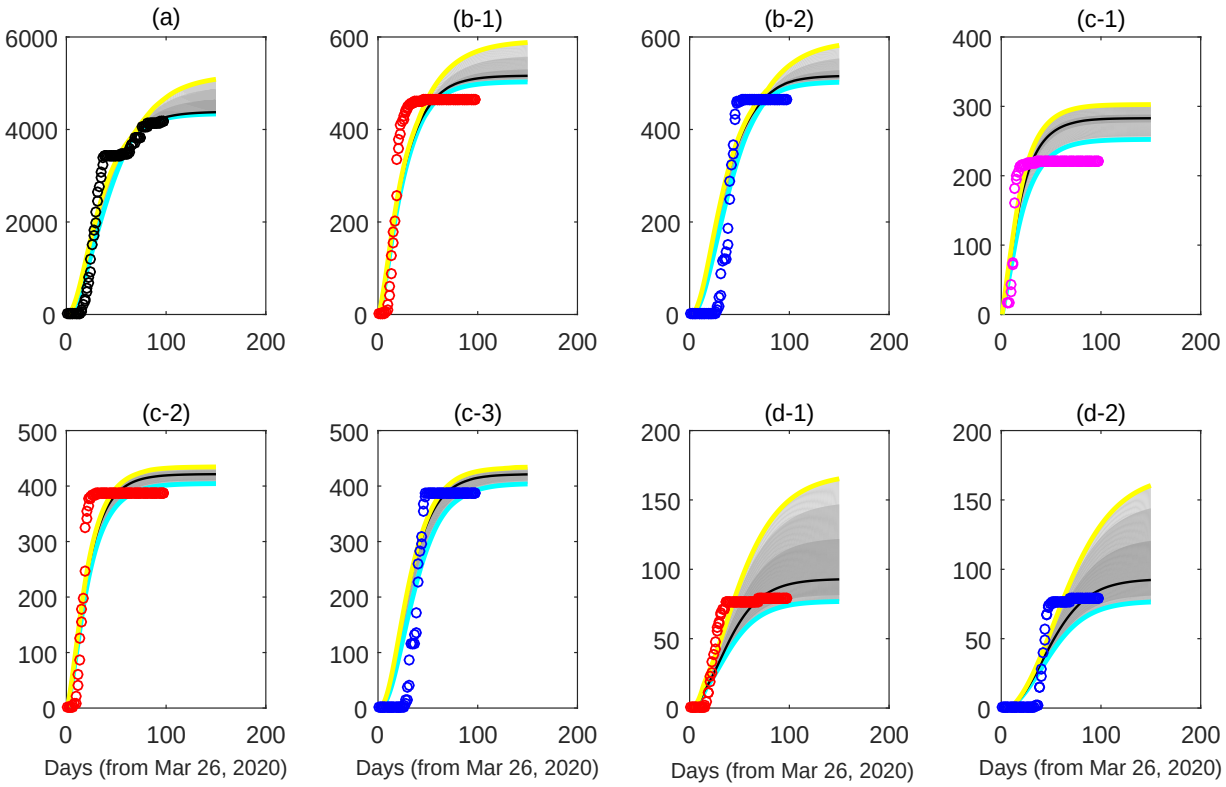

Figure 4. Goodness fitting results and validation of model (2.1) with the eight cumulative data categories from March 26 to July 1 and from July 2 to Aug 22 2020, and their 95% CI from March 26 to August 22, 2020 in Heilongjiang Province, China. The eight subplots (a), (b-1) to (b-2), (c-1) to (c-3) and (d-1) to (d-2) are the corresponding results related with the eight cumulative data in Figure 1 (a), (b), (c) and (d), respectively. The color circles are the cumulative data and the black cures are the goodness fitting results. The yellow and cyan curves denote the 95% upper and lower confidence limits.

parameter to be estimated based on their available information. That is to say, a penalized MCMC method are carried out to select the optimal parameter values and their 95% CI within the reasonable ranges which were obtained from official survey reports and previous literatures. In addition, we can obtain the basic reproduction number $R_0 = 0.7882$ for the second wave of COVID-19 in Heilongjiang Province based on the above results. Later, the values of R_0 will be as one of the important aspects to assess the effectiveness of early control strategies in the province.

3.3. Reasons for the second outbreak

The number of hiding infected individuals without effective supervision and control (*i.e.*, $E_1 + E_2 + A + I$) implies the potential transmission risk of COVID-19 epidemic from importing population. The number of infected cases in hospitals (*i.e.*, $W_F + W_D + H_F + H_D$) indicate the capacity of testing, diagnosing and treatment of the disease. The number of local infected cases in hospitals (*i.e.*, $W_D + H_D$) partly reflect the effect of illegal importing population and control strategies on the local epidemic. The number of infected individuals (*i.e.*, $E_1 + E_2 + A + I + W_F + W_D + H_F + H_D$) and the total number of cured cases (*i.e.*, R) indicate the time-varying epidemic scale and its final size, respectively. The four indexes may be used in the following parts, ordered by index 1,2,3 and 4 for simplicity.

To explore the possible reasons for the second outbreak of COVID-19 in Heilongjiang, China, we firstly assume that it is a virus-free environment in the province, so the initial values are reset as zero, besides the initial susceptible population simply fixed as its previous estimation value. The adjustment factors u_3 and u_4 reflect the protection intensity of susceptible individuals in hospitals, so their values being zero or not indicate the perfect or imperfect protection intensity. Notice that legal and illegal importing populations $(V_q^*(t), V_p^*(t))$, the percentages of illegal importing population being different subgroups $\theta_i (i = S, E_1, E_2, A, I)$ and the protection intensity $u_i (i = 3, 4)$ will impact the rebound of COVID-19 in the province. For convenience, u_3 and u_4 are fixed as the pervious estimation values to represent imperfect protection intensity. Therefore, we consider the following five special scenarios with perfect (*i.e.*, $u_3 = u_4 = 0$) or imperfect (*i.e.*, $u_i \neq 0, i = 3, 4$) protection intensity.

Case 1: No importing from aboard, *i.e.*, $V_p^*(t) = 0, V_q^*(t) = 0$;
Case 2: Only susceptible importing from aboard, *i.e.*, $V_p^*(t) = V_p(t), V_q^*(t) = V_q(t), \theta_S = 1$;
Case 3: Only legal importing from aboard, *i.e.*, $V_p^*(t) = 0, V_q^*(t) = V_p(t) + V_q(t)$;
Case 4: Only illegal importing from aboard, *i.e.*, $V_p^*(t) = V_p(t) + V_q(t), V_q^*(t) = 0$;
Case 5: Both legal and illegal importing from aboard, *i.e.*, $V_p^*(t) = V_p(t), V_q^*(t) = V_q(t)$.

It follows from Figure 5 that there is no rebound of COVID-19 if there is no importing or only susceptible individuals import from aboard no matter with perfect protection intensity or not (Cases 1 and 2 shown by cyan and magenta curves). If all importing population choose to legally enter the border, then the perfect protection intensity will not cause the rebound of the epidemic, while the imperfect protection intensity will lead to the slight rebound on the number of infected individuals under supervision or not, with the peak values at about 32 days and 50 days around 7 cases, respectively (Case 3 shown by blue curves in Figure 5). However, if all importing population illegally enter the border, the peak values of infected individuals under supervision or not at about 12 or 15 days will increase over seven times compared with the peak values in Case 3 with imperfect protection intensity (Case 4 shown by red curves in Figure 5). For the general case 5, if there are both ileal and illegal importing populations as the previous estimation, the peak values of infected individuals under supervision or not

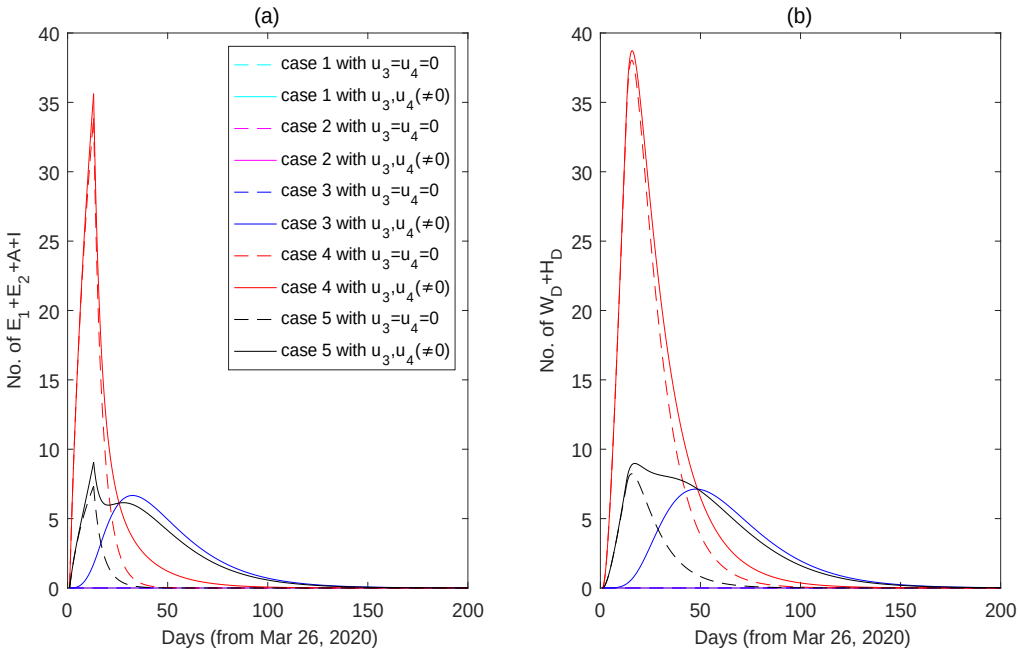

Figure 5. Possible reasons for the second outbreak of COVID-19 in Heilongjiang Province, China. The baseline parameter values are fixed as in Tables 2 and 3. Initial components are fixed as zero, except for $S_0 = 18854$.

at about 14 or 16 days will increase less than 1.5 times compared with the peak values in case 3 with imperfect protection intensity (see black curves in Figure 5). Especially, in Case 4 (or 5), there exist slightly differences on the solution curves between perfect and imperfect protection intensity around 20 (or 15) days before, then the differences of solution curves will gradually increase and then gradually decreased. All the black curves represent the baseline solutions according our previous parameter estimation. Thus the illegal importing population and imperfect protection intensity are the main reasons for the second outbreak of COVID-19 epidemic in the province.

3.4. Effectiveness of early control strategies

The early border control strategies mainly consist of the coercive government interventions, such as intensive contact tracing and quarantine q, testing and diagnosing infected cases $m_i (i = E_2, A, I)$, border closure strategy and individual compliance intensity, including wearing a mask and keeping social distance to change the contract rate c and varying the number of illegal and legal importing populations $V_i(t)(i = p, q)$. So those parameter values can used to depict the intensity of early border control strategies. In fact, the estimation of those parameter in subsection 3.2 determines the actual intensity of early border control strategies. In order to investigate whether the early border control strategies in the province are effective or not, we first regard them as the baseline situation. In Figures S1, S2, S3, S4 and S5, we compare the effects of both strengthening and weakening those parameter values with the baseline situation on the values of the four indexes, which can assess the effectiveness of controlling COVID-19 epidemic. In addition, model (2.1) involves the border control strategies. According to the definition of the basic reproduction number R_0, its value can be used to assess the

disease transmission risk and the effectiveness of control strategy in the early stage. By using the parameter estimation values and the known parameter values, we obtain $R_0 = 0.7882 < 1$ for the second wave of epidemic, which also indicates the effectiveness of its early control strategy.

In summary, it follows from either the basic reproduction number or Figures S1, S2, S3, S4 and S5 that the actual border control intensities in Heilongjiang Province are relative effective in the early border control stage, and the rebound of COVID-19 epidemic will be worsen once the actual border control strategies are relaxed. See Appendix B for more details about the explanation each one of Figures S1, S2, S3, S4 and S5.

3.5. Possible risk for long-term border closure

The COVID-19 epidemic in China has been effectively restrained due to effective control strategies adopted by the Chinese government and the better individual compliance on wearing masks and keeping social distance to degrade exposure rate, while some epidemic in the neighbouring countries, such as Russia may not yet controlled or even get worse. Then the fear to the epidemic will make more Chinese people study or working in Russia seek for a safer region by entering China through Suifenhe port in Heilongjiang Province. However, the long-term border closure in the port will further lead to more people deciding to take risks and enter illegally. Also compared with legal imported cases, illegal imported cases are much harder to be monitored in time which may greatly increase the potential spreading risk of the epidemic. Moreover, the proportions of infected importing individuals may be increased for the severity of epidemic in the neighbouring countries. It is critical to answer whether a long-term border closure may cause a paradox phenomenon or not, in other words, whether it will be much harder to block the epidemic for a long-term border closure than that for a border reopening. To depict the long-term border closure, the maximum number of illegal importing population and the proportions of them being different subgroups $\theta_i (i = S, E_1, E_2, A, I)$ are redefined by regulation parameters $f_i (i = p, q)$ and f_θ in phase III. It is difficult to obtain their accurate parameter values. Since we aim to explore the potential risks for the long-term border closure, the regulation parameters are fixed as $f_i = 4 (i = p, q)$ and $f_\theta = 3$ for simplicity. Thus we consider the following eight special scenarios along with different switching time T_2 (= 103, 163, 223), as shown in Table 4 and Figure 6.

Table 4. Eight special scenarios for the long-term border control strategies.

Case	I: $T_0 \le t < T_1$	II: $T_1 \le t < T_2$	III: $t \ge T_2$	SVF	SVC	SV
1	open with legal and illegal importing, *i.e.*, $V_p^* = V_p$, $V_q^* = V_q$	strictly close, *i.e.*, $V_p^* = V_q^* = 0$	strictly close, $V_p^* = V_q^* = 0$	0	0	0
2			close, $\hat{\alpha}_p = \hat{\alpha}_q = 0.8, V_p^* = V_p + V_q$	152.6	334.0	486.6
3			close, $\hat{\alpha}_p = \hat{\alpha}_q = 0.4, V_p^* = V_p + V_q$	456.8	1001.0	1457.8
4			close, $\hat{\alpha}_p = \hat{\alpha}_q = 0, V_p^* = V_p + V_q$	761.1	1668.0	2429.1
5			open, $V_p^* = 0, V_q^* = V_p + V_q$	107.5	1635.4	1743.0
6			open, $V_p^* = V_p, V_q^* = V_q$	278.6	1645.5	1924.2
7		open, $V_p^* = 0, V_q^* = V_p + V_q$	open, $V_p^* = 0, V_q^* = V_p + V_q$	107.5	1635.4	1743.0
8		open, $V_p^* = V_p, V_q^* = V_q$	open, $V_p^* = V_p, V_q^* = V_q$	278.6	1645.5	1924.2

SVF: the steady value of infected individuals without supervision (or with freedom), *i.e.*, $E_1 + E_2 + A + I$; SVC: the steady value of infected individuals with supervision (or with control) in hospitals, *i.e.*, $W_F + W_D + H_F + H_D$; SV: the steady value of infected individuals, *i.e.*, $E_1 + E_2 + A + I + W_F + W_D + H_F + H_D$.

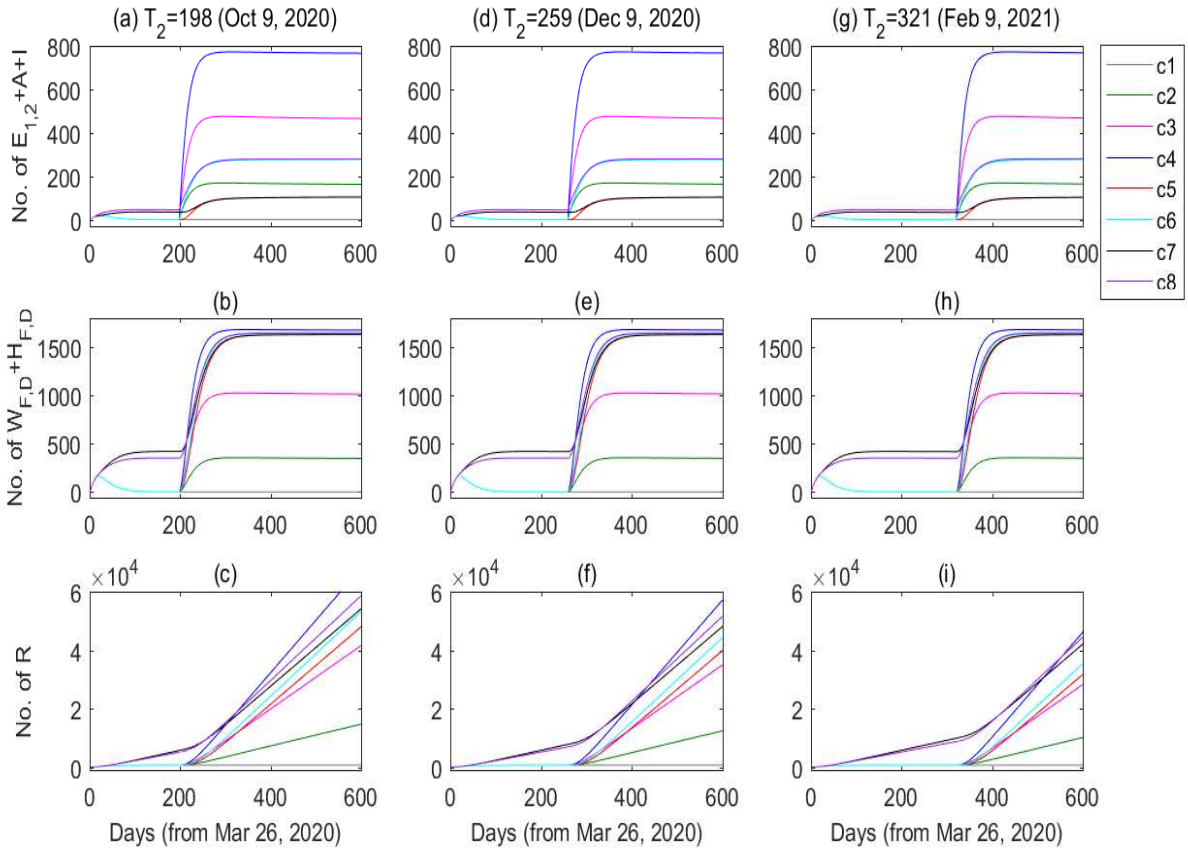

Figure 6. The evaluation of a long-term border closure on COVID-19 epidemic in Heilongjiang Province, China. (a-c): $T_2 = 198$ (Oct 9, 2020); (d-f): $T_2 = 259$ (Dec 9, 2020); (g-i): $T_2 = 321$ (Feb 9, 2021). The magenta, blue, red, cyan brown and black curves represent the corresponding solution curves of model (2.1) for the eight cases. In this work, the items $E_{1,2}$ and $W_{F,D}$ denote $E_1 + E_2$ and $W_F + W_D$, respectively. The baseline parameter values and initial values are the same as in Tables 1, 2 and 3.

From Figure 6(a)–(c) and Table 4, there are eight cases for the solutions of the three indicators in phases I, II and III. In phase II, it is clear that the strict border closure greatly contributes to prevent the COVID-19 epidemic. A sustained and strict border closure in phase III will effectively suppress the disease transmission. And SVF and SVC will greatly increase with reducing individual compliance $(\hat{\alpha}_p, \hat{\alpha}_q)$ on border closure in phase III. For some cases in phase III, SVF of border closure are larger than that of border reopening (see Table 4 and Figure 6(a)). Compared with border reopening, the existence of a paradox phenomenon in the long-term border closure not only may not help to suppress the epidemic, but worsen the epidemic control. Comparing SVC and SV among cases 2 to 8, the border reopening will greatly increase the infected individuals and then the required hospital beds and other medical resources. Moreover, there are the same SVF, SVC and SV for cases 5 and 7 due to the model (2.1) in phase III being the same with slight difference of initial values, and similar situation for cases 6 and 8. The three switching time T_2 in the simulations are chosen within the steady interval of phase II, so for model 2.1 in phase III there are the same initial values, except for the initial state of recovery

being independent to other variables. Actually the solution curves in Figures 6(d) and (e) (or (g) and (h)) are those in (a) and (b) moved forward by 2 (or 4) months. Especially, the actual SAV, SVC and SV should be correspondingly within their intervals determined by the two extreme cases 4 and 6. Although we may not know the actual switching time T_2, it can still help us to uncover the potential transmission risk and assess the final size, and then to make some advance preparations.

3.6. Border reopening measure under resource limitations

According to subsection 3.5, a long-term border closure will not only cause huge economic losses, but also may bring much severer challenges on the control of COVID-19 epidemic in Heilongjiang Province than that of border reopening with the worsening epidemic and people fearing to the epidemic in Russia. Next we will explore how to effectively reopen Suifenhe port in Heilongjiang Province.

Since anti-epidemic resources, including the number of hotel rooms and hospital beds are usually limited. In order to carry out orderly border reopening strategy, the potential required resources for importing population per day should be satisfied by the local resources. That is to say, the number of importing population per day should be determined by the locally available resources. For convenience, Φ_q and Φ_h denote the total number of hotel rooms and the total number of hospital rooms, respectively, while H_1 or H_2 denote the average maximum number of people who can be legally imported per day due to limiting resources on hotel rooms or hospital rooms, respectively. Notice that η^{-1} and $\max\{1/r_W + 1/h, 1/r_H\}$ represent the average duration of importing population being quarantined and the average duration of infected cases being treated in hospitals, respectively. Then $\Phi_q\eta$ and $\Phi_h/\max\{\frac{1}{r_W} + \frac{1}{h}, \frac{1}{r_H}\}$ are the total available numbers of hotel rooms and hospital beds per day, respectively. The items

$$\frac{qcS\Pi}{N} \text{ and } m_{E2}E_2 + m_AA + m_II + v_DQ_D$$

correspondingly represent the numbers of hotel rooms and hospital beds being used per day. Notice that

$$\frac{qcS\Pi}{N} \approx New_{quar}(t) \text{ and } m_{E_2}E_2 + m_AA + m_II + v_DQ_D \approx New_{hosp}(t), \tag{3.2}$$

where $New_{quar}(t)$ and $New_{hosp}(t)$ denote the daily new being quarantined and treated cases, respectively. The item $(k_W + k_H)v_FQ_F$ represents the daily number of required hospital rooms. Based on the resource limitations on hotel or hospital rooms, the average maximum number of people can be legally imported per day can be calculated correspondingly as

$$\Phi_q\eta - \frac{qcS\Pi}{N}$$

or

$$\frac{\Phi_h}{\max\{\frac{1}{r_W} + \frac{1}{h}, \frac{1}{r_H}\}} - (m_{E2}E_2 + m_AA + m_II + v_DQ_D).$$

Then we have

$$H_1 = \Phi_q\eta - \frac{qcS\Pi}{N} \tag{3.3}$$

and

$$(k_W + k_H)v_FQ_F = \frac{\Phi_h}{\max\{\frac{1}{r_W} + \frac{1}{h}, \frac{1}{r_H}\}} - (m_{E2}E_2 + m_AA + m_II + v_DQ_D). \tag{3.4}$$

Letting the right side of the sixth equation in model (2.1) equal to zero yields

$$Q_F = \frac{V_q}{(k_W + k_H + k_N\eta)v_F}. \tag{3.5}$$

By substituting (3.5) into (3.4), solving equation (3.4) with respect to V_q yields

$$H_2 \doteq V_q = \frac{k_W + k_H + k_N\eta}{k_W + k_H}\left(\frac{\Phi_h}{\max\{\frac{1}{r_W} + \frac{1}{h}, \frac{1}{r_H}\}} - (m_{E2}E_2 + m_A A + m_I I + v_D Q_D)\right). \tag{3.6}$$

To explore the threshold values of Φ_q^* and Φ_h^* such that the two anti-epidemic resources can be efficiently used, solving $H_1 = H_2$ with respect to Φ_q or Φ_h obtains

$$\begin{cases} \Phi_q^* &= \frac{H_2 + \frac{qcS\Pi}{N}}{\eta}, \\ \Phi_h^* &= \frac{\frac{H_1}{\frac{k_W+k_H+k_N\eta}{k_W+k_H}} + m_{E2}E_2 + m_A A + m_I I + v_D Q_D}{\max\{\frac{1}{r_W} + \frac{1}{h}, \frac{1}{r_H}\}}. \end{cases} \tag{3.7}$$

The relation between model (2.1) and the two data sets are shown in equation (3.2) and our model (2.1) can fit well with the eight data categories as in subsection 3.2. It is worth mentioning that the model driven calculations about H_1, H_2, Φ_q^* and Φ_h^* in equations (3.3), (3.6) and (3.7) can also be correspondingly replaced by the data driven ones via (3.2). Considering that the work in this section is a prospective study on future border reopening strategies, there is no data resources about the daily new to be quarantined and treated cases for border reopening. Thus here we choose to use the model driven calculations in our following numerical simulations.

Some infected individuals may enter into the border, *i.e.*, $k_W + k_H \neq 0$, if pre-entry testing is not mandatory or testing accuracy is imperfect. Then we define the daily number of people allowed to legally enter the border as

$$V_q(t) = \begin{cases} wH_1, if\ \min\{H_1, H_2, H_2 - H_1\} > 0, \\ wH_2, if\ \min\{H_1, H_2, H_1 - H_2\} > 0, \\ 0, otherwise, \end{cases} \tag{3.8}$$

where w is an adjustment factor to avoid anti-epidemic resources crowding due to some unforeseen circumstances in practice. The proportion of daily number of illegal importing population to that of legal ones is denoted by q_v, then we have

$$V_p(t) = \begin{cases} q_v wH_1, if\ \min\{H_1, H_2, H_2 - H_1\} > 0, \\ q_v wH_2, if\ \min\{H_1, H_2, H_1 - H_2\} > 0, \\ V_{p0}, otherwise. \end{cases} \tag{3.9}$$

Especially, all legal importing individuals are susceptible, *i.e.*, $k_W + k_H = 0, k_N = 1$, if pre-entry testing is mandatory and testing accuracy is perfect. Then we define the daily number of people entering the border legally or illegally as

$$V_q(t) = \begin{cases} wH_1, if\ H_1 > 0, \\ 0, otherwise, \end{cases} \quad V_p(t) = \begin{cases} q_v wH_1, if\ H_1 > 0, \\ V_{p0}, otherwise. \end{cases} \tag{3.10}$$

In order to explore the effects of the proportion of legal importing population being susceptible k_N, the number of illegal importing population $V_p(t)$, the regulatory factors of contact rates from protecting compliance in hospitals $u_i(i = 3, 4)$, initial values (depicted by P_0) and anti-epidemic resources $\Phi_i(i = q, h)$ on the potential transmission risk and the occupied number of hospital beds when the border reopening strategy is carried out in Suifenhe port. We analyze the sensitivity for varying one, two and three of the above control parameters $(k_N, V_p(t), u_i)$ separately based on the designed reopening strategy, as shown in Figures 7, 8 and 9. According to the news reports about the numbers of hospital rooms and medical beds on Suifenhe, the two resource parameters are set as $\Phi_q = 939$ and $\Phi_h = 630$. All parameter values are the same as our previous estimations, except for the above noteworthy ones. Specifically in Figures 7 and 8, besides of the target parameters, other noteworthy ones are fixed as $k_N = 1, V_p = u_3 = u_4 = 0$, and the initial values are fixed as zero, except for $S_0 = 18854$. In Figure 9, besides of the target parameters, other noteworthy ones are fixed as $k_N = 0.9, V_p = 0.05V_q, u_i = 0.2\hat{u}_i(i = 3, 4)$ and $P_0 = 10$, where $\hat{u}_i$ are the estimation values of u_i in Table 2.

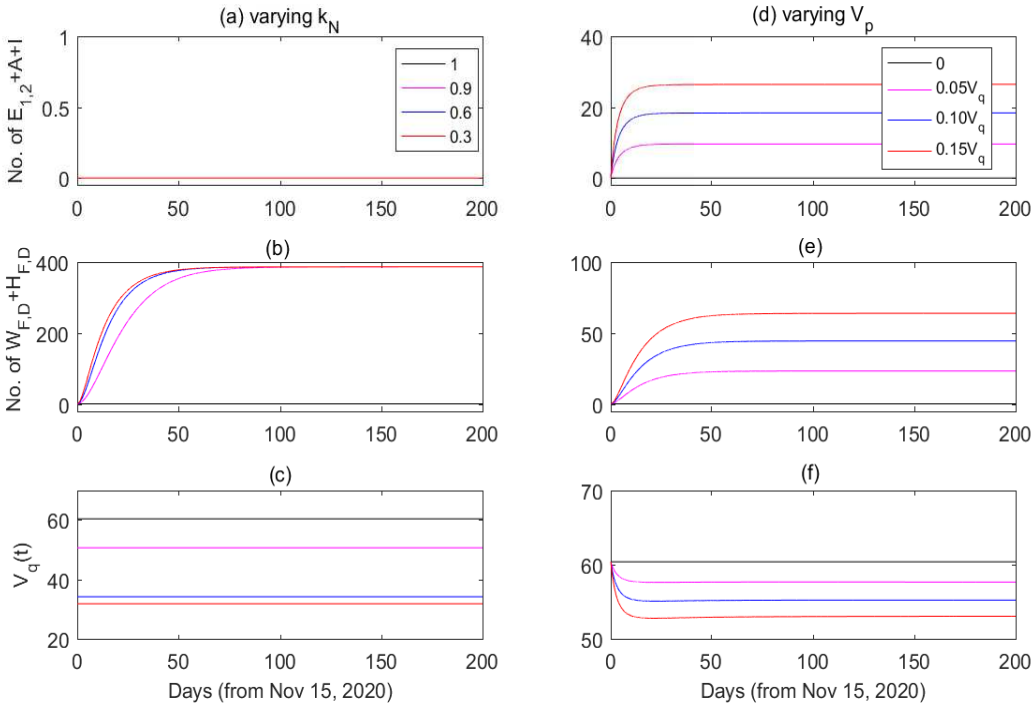

Figure 7. Effects of varying one control parameter value (k_N or $V_p(t)$) on the border reopening of Suifenhe prot in Heilongjiang Province, China. (a-c): $V_p = u_3 = u_4 = 0$; (d)-(f): $k_N = 1, u_3 = u_4 = 0$. The initial values and baseline parameter values are the same as in Figures 5, and $\Phi_q = 939, \Phi_h = 630$.

Although there is no potential transmission risk, no occupied medical beds and a high number of legal importing population for border reopening with ideal situations *i.e.*, $k_N = 1, V_p = u_3 = u_4 = 0$ (see black curves in Figure 7 (a-b) and (d-e)), it is difficult to simultaneously attain those perfect control intensities in reality. There is the same results for $k_N = 1, V_p = 0$ and $u_i \neq 0(i = 3, 4)$, so here we do not show its simulation results. From Figure 7 (a-c), no illegal importing together with perfect protection intensity $V_p = u_3 = u_4 = 0$ can successfully suppress the potential transmission risk even

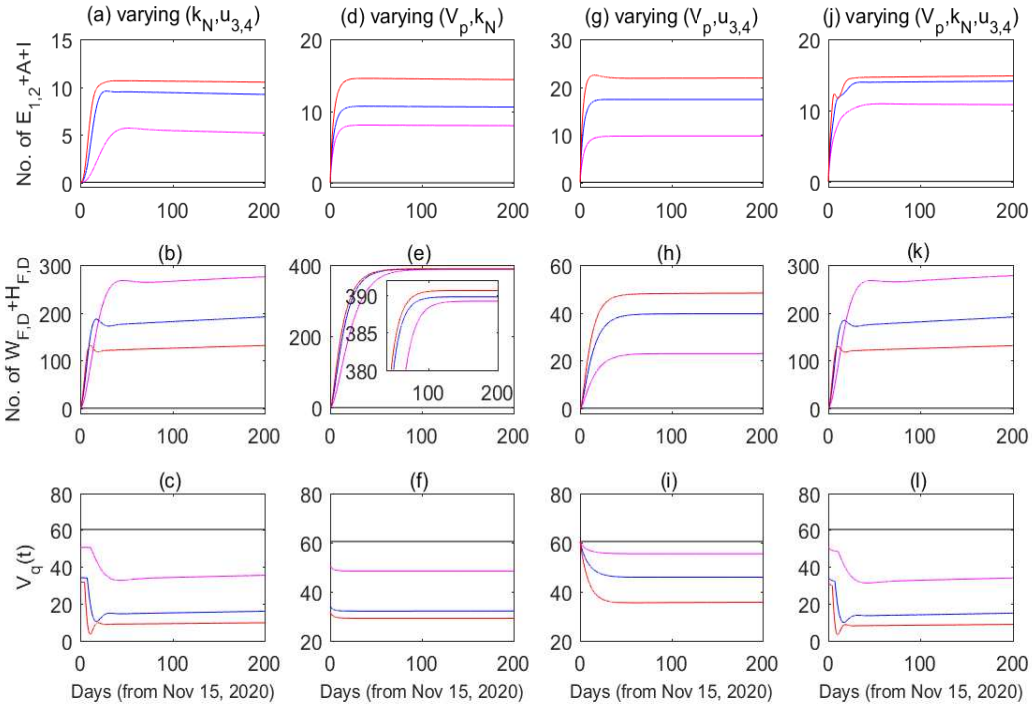

Figure 8. Effects of varying two or three control parameter values ($V_p(t)$,k_N,$u_{3,4}$) on the border reopening strategy of Suifenhe prot in Heilongjiang Province, China. The black, magenta, blue and red solution curves in (a-c) for $(1, u_{3,4})$, $(0.9, 0.2u_{3,4})$, $(0.6, 0.5u_{3,4})$ and $(0.3, 0.8u_{3,4})$; in (d-f) for $(0, 1)$, $(0.05V_q, 0.9)$, $(0.1V_q, 0.6)$ and $(0.15V_q, 0.3)$; in (g-i) for $(0, u_{3,4})$, $(0.05V_q, 0.2u_{3,4})$, $(0.1V_q, 0.5u_{3,4})$ and $(0.15V_q, 0.8u_{3,4})$, and in (j-l) for $(0, 1, u_{3,4})$, $(0.05V_q, 0.9, 0.2u_{3,4})$, $(0.1V_q, 0.6, 0.5u_{3,4})$ and $(0.15V_q, 0.3, 0.8u_{3,4})$. The initial values and baseline parameter values and are the same as in Figures 5.

for legal importing population with high infection proportion (i.e., low k_N). Also the increase of k_N can help to reduce the occupied number of medical beds in the first two months followed by tending to the same steady values, and help to increase the daily number of legal importing population for border reopening. From Figure 7 (d-f), the lower V_p is benefit to reduce the potential transmission risk and the number of occupied medical beds, and increase the daily number of legal importing population. The improvement for control intensities through combining two or three parameters (here V_p, k_N, u_i) at the same time can help to reduce the potential transmission risk and increase the daily number of legal importing population to some extent, see Figure 8. In reality, on the one hand, we aim to reduce the potential transmission risk and increase the number of legal importing population by improving control intensities; on the other hand, the quantity of infected population under supervision should be lower than the available medical beds to receive infected individuals in time, although there is no consistent conclusion for its quantity with improving control intensities, see Figures 8.

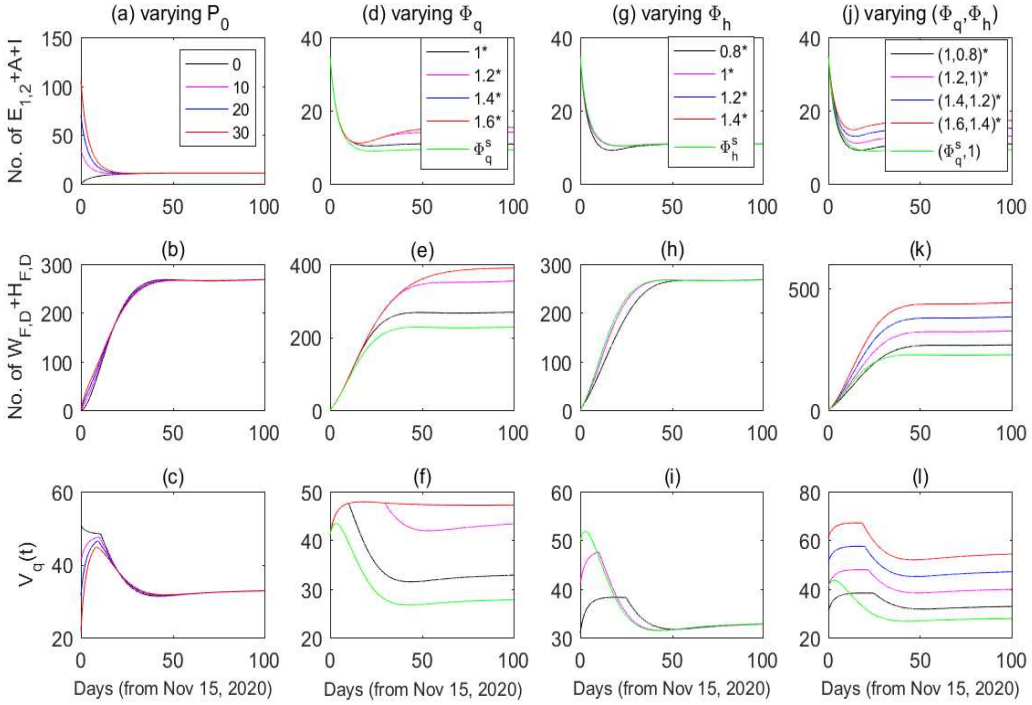

Figure 9. Effects of varying initial values reflected by P_0 and anti-epidemic resources $\Phi_i (i = q, h)$ on the border reopening strategy of Suifenhe prot in Heilongjiang Province, China. Fix $E_{10} = E_{A0} = E_{I0} = P_0$, $E_{20} = 0.5P_0$ and $P_0 = 10$ in (d-l). In (d)-(f), $1.2*$ represents Φ_q replaced by $1.2\Phi_q$; in (j)-(i), $(1.4, 1.2)*$ represents Φ_q and Φ_h replaced by $1.4\Phi_q$ and $1.2\Phi_h$, respectively. There are similar meanings for other items. The baseline parameter values and are the same as in Figures 5.

It follows from Figure 9, varying the values of P_0 and Φ_h can only impact the solution curves in the earlier phase followed by tending to the same steady values. The stable solution curves for different values of Φ_h coincide with the stable curves for the threshold values Φ_h^S (green) in Figure 9 (g-i). From Figure 9 (d-f), the stable solution curves for the estimation values (black) is higher than that for the threshold values Φ_q^S (green), and the corresponding stable solution curves will increase with increasing

Φ_q from 1 to 1.2, 1.4 multiplying by the actual hotel room number 939. However, the stable solution curves will not been changed with unceasingly increasing the values of Φ_q from 1.4 to 1.6, times 939. It indicates that in Suifenhe port, the quantity of actual available medical beds is more sufficient than that of required ones compared with the required and available quantities of hotel rooms, and that there will no help to reduce the potential transmission risk or increase the number of legal importing population when successively increasing available hotel rooms make its number more than that of required ones. In Figures 9 (j-l), the stable solution curves will increase with simultaneously increasing the hotel room and medical bed numbers. Compared with Figures 9 (d-i), the simultaneously increasing the anti-epidemic resources can only make a slight addition on the number of infected individuals without supervision, but can help to increase the numbers of both infected individuals in hospitals and legal importing population. It is worth mentioning that with increasing the hotel room number or medical bed number based on the designed border reopening strategy, the quantity of the available medical beds is always more than that of infected individuals under supervision, even when the number of infected individuals may be increased to some extent, and that the allowable number of legal importing population is increased. Hence, the designed border reopening process give an effective strategy of reopening Suifenhe port with considering limitation resources.

4. Conclusions

The local transmission of COVID-19 seems to have been contained in China under unprecedented public health interventions, while some epidemics in the neighbouring countries, such as Russia may not yet controlled or even getting worse. The second wave of outbreak was aroused in several regions owing to introducing some imported cases, such as Heilongjiang, Beijing and so on. Especially, Suifenhe port of Heilongjiang Province undertook major imported cases after the strict policy of immigration diversion in main entry ports by the government, and then the severe rebound of the epidemic occurred in the province. It is necessary to investigate all possible reasons for the second outbreak of the disease, and assess the effects of early border control strategies on the prevention of the disease. It is intuitive that border closure in Suifenhe prot contributes to the restrain the rebound of epidemic in the provinces. However, the fear to the severity of epidemic in Russia could make more people seek for a safer region by illegally entering Heilongjiang Province, China, which could be worsen if a long-term border closure will carry out in the border port. And illegal imported cases may greatly increase the potential spreading risk of the epidemic since they are much harder to be monitored in time. It is critical to explore the possible risk for the long-term border closure strategy, and then design an effective border reopening measure with considering the limitation of anti-epidemic resources. To answer above relative issues, we developed a time switching system to depict the transmission and spread of COVID-19 in three different time phases. The daily numbers of legal and illegal importing populations and the percentages of illegal importing population are depicted in three phases by introducing several adjustment parameters. The basic reproduction number are calculated as in (3.1), which can be separated into five parts from the possible types of infected individuals. Notice that there were no new or suspected infected cases for Heilongjiang Province and all confirmed cases have been cured on March 26 and July 1, 2020, so the eight data categories in this duration are chosen to study the effects of imported cases on the COVID-19 rebound and its control in the province. Cross validation was carried out by fitting the model with eight time series of cumulative numbers simultaneously to

improve the credibility of parameter estimation values. And a penalized MCMC method are carried out such that the optimal parameter value and 95% CI lie in its reasonable priori distribution for each parameter. Comparing five special scenarios under perfect and imperfect protection intensity, we have shown that illegal importing cases and imperfect protection intensity in hospitals are the main reasons for the rebound of the epidemic.

The intensity of early border control strategy is mainly determined by parameter values of government intervention and individual compliances (here $q, m_*, T_1, c, V_p(t)$ and $V_q(t)$). So the sensitive analysis are done by comparing the solutions of the four indicator via strengthening or weakening the estimation value of target parameters. Simulations show that the actual border control intensities for the province in the early control stage are relatively effective, while the rebound of the epidemic will be worsen once the strategies are relaxed and vice versa. However, we find that a long-term border closure may cause a paradox phenomenon such that it is much harder to control the epidemic as shown in Table 4 and Figure 6.

Combining with reducing the number of legal population, decreasing the proportion of legal population being infected via improving test rates and accuracy and turning time, and improving protection compliance in hospitals, we design a border reopening strategy to avoid the paradox for long-term border control strategies by balancing the limited resources on hotel rooms for quarantine and hospital beds. Goodness fitting results show that our model can well describe the disease transmission in Heilongjiang Province. And assume that each hotel room or hospital bed corresponds to one being quarantined or treated case. Then the daily new being quarantined and treated cases driven by actual data should approximately equal to the daily number of hotel rooms and hospital beds being used driven by the model. The choice for the definitions of H_1 and H_2 following by $V_q(t)$ and $V_p(t)$ are determined by whether the actual data of daily new quarantined and treated cases can be obtained or not. In this work, we choose the model driven definitions since it is a prospective study on future border reopening strategies. In fact, we can also use the current data to timely forecast the allowed number of legal importing population on the next day. By the border reopening measure, we could estimate the daily reasonable number of legal importing population by considering the resource limitations, which could inform public health decision-makers carrying out the better border reopening strategy. It should be mentioned that our results will not only help to contain the spread of the epidemic in the province, but also can be referred for epidemic control in other regions or countries for border control with imported cases.

Conflict of interest

The authors declare that we have no conflict of interest.

Acknowledgements

This work is supported by the National Natural Science Foundation of China (NSFC, 12001448), the Doctoral Fund of Southwest University (No. SWU019046) and Natural Science Foundation of Chongqing (cstc2020jcyj-msxmX0432). This work is also supported by the Canadian Institutes of Health Research(CIHR), Canadian COVID-19 Math Modelling Task Force, the Natural Sciences and Engineering Research Council (NSERC) of Canada and York University Research Chair program.

References

1. Sina News. Update on the outbreak of Covid-19 at 24:00, 18 March, 2020. Available from: http://news.sina.com.cn/zx/2020-03-19/doc-iimxxsth0137436.shtml (accessed on 18 Mar 2020).
2. Heilongjiang Daily. CCTV news 1+1: focuses on Suifenhe, China, 2020. Available from: Http://www.hlj.gov.cn/zwfb/system/2020/04/14/010923836.shtml (accessed on 14 Apr 2020).
3. CAAC. Notice on the continued reduction of international passenger flights during the epidemic prevention and control period, 2020. Available from: http://www.caac.gov.cn/XXGK/XXGK/TZTG/202003/t20200326_201746.html (accessed on 26 Mar 2020).
4. CAAC. Notice of civil Aviation Administration on adjustment of international passenger flights, Civil aviation administration of China, 2020. Available from: http://www.caac.gov.cn/XXGK/XXGK/TZTG/202006/t20200604_202928.html (accessed on 4 Jun 2020).
5. Sina News. The Civil Aviation Administration responded that international flights have been redirected to 12 entry points: Beijing Airport has more than 200 inbound flights from 33 countries every week, 2020. Available from: http://finance.sina.com.cn/roll/2020-03-23/doc-iimxxsth1242997.shtml (accessed on 23 Mar 2020).
6. Heilongjiang Municipal Government. The Suifenhe-Bologanichny Port Passenger Inspection Channel was temporarily closed, 2020. Available from: https://www.hlj.gov.cn/n200/2020/0408/c35-10923381.html (accessed on 8 Apr 2020).
7. Suifenhe Municipal People's Government. Notice No.19 of Suifenhe Epidemic Prevention and Control Headquarters, 2020. Available from: http://www.suifenhe.gov.cn/contents/1962/80492.html (accessed on 9 Apr 2020).
8. Suifenhe Municipal People's Government. Document No.9:Suifenhe City shall respond to the control measures of 'Nine Stricts and One Protection' for CoviD-19 epidemic prevention and export prevention and control, 2020. Available from: http://www.suifenhe.gov.cn/contents/1962/80547.html (accessed on 12 Apr 2020).
9. Suifenhe Municipal People's Government. Suifenhe epidemic prevention and control headquarters twenty-first notice, 2020. Available from: http://www.suifenhe.gov.cn/contents/1962/80548.html (accessed on 12 Apr 2020).
10. Heilongjiang Public Security Department. Heilongjiang issued Notice No.14: The first place of entry is the place of quarantine, 2020. Available from: https://mp.weixin.qq.com/s/FXArnr4pyo9qAXUgsH5leA (accessed on 2 Apr 2020).
11. Health Commission of Heilongjiang Province. Latest outbreak report, 2020. Available from: http://wsjkw.hlj.gov.cn/pages/5fd2a7e712c15bde3d36385a (accessed on 11 Dec 2020).
12. Health Commission of Heilongjiang Province. Latest outbreak report, 2021. Available from: http://wsjkw.hlj.gov.cn/pages/6008c1ff12c15b4f69f68e3c (accessed on 21 Jan 2020).
13. X. Yu, Modelling Return of the Epidemic: Impact of Population Structure, Asymptomatic Infection, Case Importation and Personal Contacts, *Travel Med. Infect. Di.,* **37** (2020), 1–8. doi: 10.1016/j.tmaid.2020.101858.

14. M. Kraemer, C. Yang, B. Gutierrez, C. H. Wu, B. Klein, D. M. Pigott, et al., The effect of human mobility and control measures on the COVID-19 epidemic in China, *Science,* **368** (2020), 493–497. doi: 10.1126/science.abb4218.

15. H. Sun, B. Dickens, A. Cook, H. Clapham, Importations of COVID-19 into African countries and risk of onward spread, *BMC Infect. Dis.,* **20** (2020), 1–13. doi: 10.1186/s12879-020-05323-w.

16. T. Sun, D. Weng, Estimating the effects of asymptomatic and imported patients on COVID-19 epidemic using mathematical modeling, *J. Med. Virol.,* **92** (2020), 1995–2003. doi: 10.1002/jmv.25939.

17. Z. Hu, Q. Cui, J. Han, X. Wang, E. Wei, Z. Teng, Evaluation and prediction of the COVID-19 variations at different input population and quarantine strategies, a case study in Guangdong province, China, *Int. J. Infect. Dis.,* **95** (2020), 231–240. doi: 10.1016/j.ijid.2020.04.010.

18. M. Hossain, A. Junus, X. Zhu, P. Jia, T. Wen, D. Pfeiffer, et al., The effects of border control and quarantine measures on the spread of COVID-19, *Epidemics* **32** (2020), 100397. doi: 10.1016/j.epidem.2020.100397.

19. T. Chen, J. Rui, Q. Wang, Z. Zhao, J. Cui, L. Yin, A mathematical model for simulating the phase-based transmissibility of a novel coronavirus, *Infect. Dis. Poverty,* **9** (2020), 1–8. doi: 10.1186/s40249-020-00640-3.

20. I. Coopera, A. Mondal, C. Antonopoulos, Dynamic tracking with model-based forecasting for the spread of the COVID-19 pandemic, *Chaos Soliton. Fract.,* **139** (2020), 110298. doi: 10.1016/j.chaos.2020.110298.

21. Q. Li, Y. Xiao, J. Wu, Modelling COVID-19 epidemic with time delay and analyzing the strategy of confirmed cases-driven contact tracing followed by quarantine, *Acta Math. Appl. Sin.,* **43** (2020), 238–250. (in Chinese)

22. L. Zou, S. Ruan, A patch model of COVID-19: the effects of containment on chongqing, *Acta Math. Appl. Sin.,* **43** (2020), 310–323. (in Chinese)

23. H. Loeffler-Wirth, M. Schmidt, H. Binder, Covid-19 transmission trajectories−monitoring the pandemic in the worldwide context, *Viruses,* **12** (2020), 777. doi: 10.3390/v12070777.

24. J. Hellewell, S. Abbot, A. Gimma, N. Bosse, C. Jarvis, T. Russell, et al., Feasibility of controlling COVID-19 outbreaks by isolation of cases and contacts, *Lancet Glob. Health,* **8** (2020), e488–e496. doi: 10.1016/S2214-109X(20)30074-7.

25. G. Giordano, F. Blanchini, R. Bruno, P. Colaneri, A. Di Filippo, A. Di Matteo, et al., Modelling the COVID-19 epidemic and implementation of population-wide interventions in Italy, *Nat. Med.,* **26** (2020), 855–885. doi: 10.1038/s41591-020-0883-7.

26. S. Saha, G. Samanta, J. Nieto, Epidemic model of COVID-19 outbreak by inducing behavioural response in population, *Nonlinear Dynam.,* **102** (2020), 455–487. doi: 10.1007/s11071-020-05896-w.

27. F. Ndaïrou, I. Area, J. Nieto, D. Torres, Mathematical modeling of COVID-19 transmission dynamics with a case study of Wuhan, *Chaos Soliton. Fract.,* **135** (2020), 109846. doi: 10.1016/j.chaos.2020.109846.

28. K. Bubar, K. Reinholt, S. Kissler, M. Lipsitch, S. Cobey, Y. Grad, et al., Model-informed COVID-19 vaccine prioritization strategies by age and serostatus, *Science,* **371** (2021), 916–921. doi: 10.1126/science.abe6959.

29. C. Kerr, R. Stuart, D. Mistry, R. Abeysuriya, K. Rosenfeld, G. Hart, et al., Covasim: an agent-based model of COVID-19 dynamics and interventions, *PLOS Comput. Biol.,* **17** (2021), e1009149. doi: 10.1371/journal.pcbi.1009149.

30. I. Baba, A. Yusuf, K. Nisar, A. Abdel-Aty, T. Nofal, Mathematical model to assess the imposition of lockdown during COVID-19 pandemic, *Results Phys.,* **20** (2021), 103716. doi: 10.1016/j.rinp.2020.103716.

31. S. Nadim, I. Ghosh, J. Chattopadhyay, Short-term predictions and prevention strategies for COVID-19: a model-based study, *Appl. Math. and Comput.,* **404** (2021), 126251. doi: 10.1016/j.amc.2021.126251.

32. P. Driessche, J. Watmough, Reproduction numbers and sub-threshold endemic equilibria for compartmental models of disease transmission, *Math. Biosci.,* **180** (2002), 29–48. doi: 10.1016/s0025-5564(02)00108-6.

33. Q. Li, B. Tang, N. Bragazzi, Y. Xiao, J. Wu, Modeling the impact of mass influenza vaccination and public health interventions on covid-19 epidemics with limited detection capability, *Math. Biosci.,* **325** (2020), 108378. doi: 10.1016/j.mbs.2020.108378.

34. B. Tang, X. Wang, Q. Li, N. Bragazzi, S. Tang, Y. Xiao, et al., Estimation of the Transmission Risk of the 2019-nCoV and Its Implication for Public Health Interventions, *J. Clin. Med.,* **9** (2020), 462. doi: 10.3390/jcm9020462.

35. S. Tang, Z. Xu, X. Wang, X. Feng, Y. Xiao, Y. Chen, et al., When will be the resumption of work in wuhan and its surrounding areas during covid-19 epidemic? A data-driven network modeling analysis, *Scientia Sinica Mathematica,* **50** (2020), 969–978. doi: 10.1360/SSM-2020-0037

36. A. Morton, B. Finkenstadt, Discrete time modelling of disease incidence time series by using Markov chain Monte Carlo methods. Discrete time modelling of disease incidence time series by using markov chain monte carlo methods, *J. R. Stat. Soc. C-Appl.,* **54** (2005),575–594. doi: 10.1111/j.1467-9876.2005.05366.x.

37. M. Keeling, M. Tildesley, B. Atkins, B. Penman, E. Southall, GirlGuyver-Fletcher, et al., The impact of school reopening on the spread of COVID-19 in England, *Philos. T. R. Soc. B.,* **376** (2021), 20200261. doi: 10.1098/rstb.2020.0261.

Appendix

Appendix A: Equilibria and basic reproduction number

From model (2.1), variable R is independent to other variables since it does not appear in other equations. So we remove the equation related with R in model (2.1) and set the right-hand side of other equations being zero to compute the equilibria of the model. Denote the positive equilibrium as $P(S^*, E_1^*, E_2^*, A^*, I^*, Q_F^*, Q_D^*, Q_S^*, W_F^*, W_D^*, H_F^*, H_D^*)$.

We firstly obtain the expressions of Q_F^*, S^* and Q_D^* from $Q_F^{'} = 0, E_1^{'} = 0, Q_D^{'} = 0$ as follows

$$Q_F^* = \frac{(1-\varepsilon)V_q(t)}{(k_W + k_H + k_N\eta)v_F}, S^* = \frac{(-\theta_{EI}\left(V_p(t) + \varepsilon V_q(t)\right) + \delta E_1^*)N^*}{(1-q)\beta c\Pi}, Q_D^* = \frac{q\beta c S^*\Pi}{v_D N^*}.$$

By adding the four equations $E_1^{'} = 0, S^{'} = 0, Q_D^{'} = 0, Q_S^{'} = 0$, we have

$$\theta_S\left(V_p(t) + \varepsilon V_q(t)\right) + \theta_{E1}\left(V_p(t) + \varepsilon V_q(t)\right) + v_F k_N \eta Q_F^* - \delta E_1^* - v_D Q_D^* = 0.$$

According to the above equations, we have

$$E_1^* = \left(\left(\theta_S + \frac{\theta_{E1}}{1-q}\right)\left(V_p(t) + \varepsilon V_q(t)\right) + \frac{(1-\varepsilon)V_q(t)k_N\eta}{k_W + k_H + k_N\eta}\right)(1-q).$$

From equations $E_2^* = 0, A^* = 0, I^* = 0$, we then obtain

$$E_2^* = \frac{\theta_{E2}\left(V_p(t) + \varepsilon V_q(t)\right) + \delta E_1^*}{\rho + m_{E2}}, A^* = \frac{\theta_A\left(V_p(t) + \varepsilon V_q(t)\right) + k_A\rho E_2^*}{r_A + m_A},$$

$$I^* = \frac{\theta_I\left(V_p(t) + \varepsilon V_q(t)\right) + (1-k_A)\rho E_2^*}{r_I + m_I}.$$

Based on $Q_S^{'} = 0, W_F^{'} = 0, W_D^{'} = 0, H_F^{'} = 0, H_D^{'} = 0$, we have

$$Q_S^* = \frac{qc(1-\beta)S^*\Pi}{\eta N^*}, W_F^* = \frac{k_W v_F Q_F^*}{r_W + h}, W_D^* = \frac{k_D v_D Q_D^* + m_{E2}E_2^* + m_A A^*}{r_W + h},$$

$$H_F^* = \frac{k_H v_F Q_F^* + hW_F^*}{r_H + d}, H_D^* = \frac{(1-k_D)v_D Q_D^* + hW_D^* + m_I I^*}{r_H + d},$$

Then the positive equilibrium of model (2.1) can be obtained by substituting E_1^* into the expressions of above components.

Next, we will calculate the effective reproduction number R_t by using the next generation matrix method [32], and then we can obtain the basic reproduction number R_0 by setting $t = 0$. According to our data collection of the province, there is no new dead case from COVID-19 during the second outbreak. Thus under the assumptions of no importing population and ignoring disease-induced death rate, there exists a disease-free equilibrium for the model. Then we first calculate the effective reproduction number R_t by using the next generation matrix method [32].

At first, we define

$$\mathscr{F} = \begin{bmatrix} \frac{((1-q)\beta+q)cS\Pi}{N} \\ 0 \\ 0 \\ 0 \\ 0 \\ \frac{qc\beta S\Pi}{N} \\ \frac{qc(1-\beta)S\Pi}{N} \\ 0 \\ 0 \\ 0 \\ 0 \\ 0 \\ 0 \end{bmatrix}, \mathscr{U} = \begin{bmatrix} \delta E_1 \\ -\delta E_1 + \rho E_2 + m_{E2} E_2 \\ -k_A \rho E_2 + r_A A + m_A A \\ -(1-k_A)\rho E_2 + r_I I + m_I I \\ -(1-\varepsilon)V_q(t) + (k_W + k_H + k_N \eta) v_F Q_F \\ v_D Q_D \\ \eta Q_S \\ -k_W v_F Q_F + r_W W_F + h W_F \\ -k_D v_D Q_D - m_{E2} E_2 - m_A A + r_W W_D + h W_D \\ -k_H v_F Q_F - h W_F + d H_F + r_H H_F \\ -(1-k_D) v_D Q_D - h W_D - m_I I + d H_D + r_H H_D \\ \frac{((1-q)\beta+q)cS\Pi}{N} - k_N v_F \eta Q_F - \eta Q_S \\ -r_A A - r_I I - r_W (W_F + W_D) - r_H (H_F + H_D) \end{bmatrix} \tag{S1}$$

Then the new infection and remaining transfer terms are given respectively by F and U as follows

$$F = \begin{bmatrix} 0 & K_1 u_2 & K_1 u_1 & K_1 & 0 & 0 & 0 & K_1 u_3 & K_1 u_3 & K_1 u_4 & K_1 u_4 \\ 0 & 0 & 0 & 0 & 0 & 0 & 0 & 0 & 0 & 0 & 0 \\ 0 & 0 & 0 & 0 & 0 & 0 & 0 & 0 & 0 & 0 & 0 \\ 0 & 0 & 0 & 0 & 0 & 0 & 0 & 0 & 0 & 0 & 0 \\ 0 & 0 & 0 & 0 & 0 & 0 & 0 & 0 & 0 & 0 & 0 \\ 0 & K_2 u_2 & K_2 u_1 & K_2 & 0 & 0 & 0 & K_2 u_3 & K_2 u_3 & K_2 u_4 & K_2 u_4 \\ 0 & K_3 u_2 & K_3 u_1 & K_3 & 0 & 0 & 0 & K_3 u_3 & K_3 u_3 & K_3 u_4 & K_3 u_4 \\ 0 & 0 & 0 & 0 & 0 & 0 & 0 & 0 & 0 & 0 & 0 \\ 0 & 0 & 0 & 0 & 0 & 0 & 0 & 0 & 0 & 0 & 0 \\ 0 & 0 & 0 & 0 & 0 & 0 & 0 & 0 & 0 & 0 & 0 \\ 0 & 0 & 0 & 0 & 0 & 0 & 0 & 0 & 0 & 0 & 0 \end{bmatrix} \tag{S2}$$

$$U = \begin{bmatrix} \delta & 0 & 0 & 0 & 0 & 0 & 0 & 0 & 0 & 0 & 0 \\ -\delta & m_{E2} + \rho & 0 & 0 & 0 & 0 & 0 & 0 & 0 & 0 & 0 \\ 0 & -k_A \rho & K_A & 0 & 0 & 0 & 0 & 0 & 0 & 0 & 0 \\ 0 & K_4 & 0 & K_I & 0 & 0 & 0 & 0 & 0 & 0 & 0 \\ 0 & 0 & 0 & 0 & K_5 & 0 & 0 & 0 & 0 & 0 & 0 \\ 0 & 0 & 0 & 0 & 0 & v_D & 0 & 0 & 0 & 0 & 0 \\ 0 & 0 & 0 & 0 & 0 & 0 & \eta & 0 & 0 & 0 & 0 \\ 0 & 0 & 0 & 0 & -k_W v_F & 0 & 0 & K_6 & 0 & 0 & 0 \\ 0 & -m_{E2} & -m_A & 0 & 0 & -k_D v_D & 0 & 0 & K_6 & 0 & 0 \\ 0 & 0 & 0 & 0 & -k_H v_F & 0 & 0 & -h & 0 & K_8 & 0 \\ 0 & 0 & 0 & -m_I & 0 & K_7 & 0 & 0 & -h & 0 & K_8 \end{bmatrix} \tag{S3}$$

with $K_1 = (1-q)\beta cS/N, K_2 = qc\beta S/N, K_3 = qc(1-\beta)S/N, K_4 = (k_A - 1)\rho, K_5 = (k_W + k_H + k_N\eta)v_F, K_6 = h + r_W, K_7 = (k_D - 1)v_D, K_8 = d + r_H, K_i = m_i + r_i, i = I, A$. Then the effective reproduction number R_t of model (2.1) is determined by $\rho(FU^{-1})$, where ρ denotes the spectral radius. Then we have

$$R_{0t} = R_{t1} + R_{t2} + R_{t3} + R_{t4} + R_{t5}, \tag{S4}$$

where

$$R_{t1} = \frac{\beta c\rho(1-k_A)(1-q)}{(m_I+r_I)(\rho+m_{E2})}\frac{S}{N}, R_{t2} = \frac{\beta c u_1 k_A \rho(1-q)}{(m_A+r_A)(\rho+m_{E2})}\frac{S}{N}, R_{t3} = \frac{\beta c u_2(1-q)}{(\rho+m_{E2})}\frac{S}{N},$$
$$R_{t4} = \frac{\beta c u_3 m_{E2}(1-q)}{(r_W+h)(\rho+m_{E2})}\frac{S}{N} + \frac{\beta c u_3 k_A m_A \rho(1-q)}{(r_W+h)(\rho+m_{E2})(m_A+r_A)}\frac{S}{N} + \frac{\beta c u_3 k_D q}{(r_W+h)}\frac{S}{N},$$
$$R_{t5} = \frac{\beta c u_4 q[\rho h + (\rho+m_{E2})(1-k_D)r_W)]}{(r_H+d)(r_W+h)(\rho+m_{E2})}\frac{S}{N} + \frac{\beta c u_4 \rho(1-q)(1-k_A)m_I}{(r_H+d)(m_I+r_I)(\rho+m_{E2})}\frac{S}{N}$$
$$+\frac{\beta c u_4 h\rho k_A(1-q)m_A}{(r_H+d)(r_W+h)(\rho+m_{E2})(m_A+r_A)}\frac{S}{N}.$$

In fact, $R_{t1}, R_{t2}, R_{t3}, R_{t4}$ and R_{t5} indicate the average number of individuals infected by the introduction of a single infected individual of I, A, E_2, W_F or W_D and H_F or H_D in the whole susceptible population respectively.

Actually the formula of R_t is a function with respect to time t, and it exists the term $S(t)/(N(t)$. Then we can directly obtain the formula of R_0 by setting $t = 0$ in Eq. (S4). Note that in the beginning of the disease rebound, it is reasonable to assume that the initial number of susceptible population (*i.e.*, $S(0)$) would approximate to the number of total populations (*i.e.*, $N(0)$), then the term $S(0))/(N(0)$ can be simplified as one. So we can obtain R_0 by removing the term S/N in Eq. (S4).

Appendix B: Effectiveness of early control strategies

In Figures S1, S2, S3, S4 and S5, we compare the effects of both strengthening and weakening those parameter values with the baseline situation on the values of the four indexes, which can assess the effectiveness of early control strategies of COVID-19 epidemic in Heilongjiang Province.

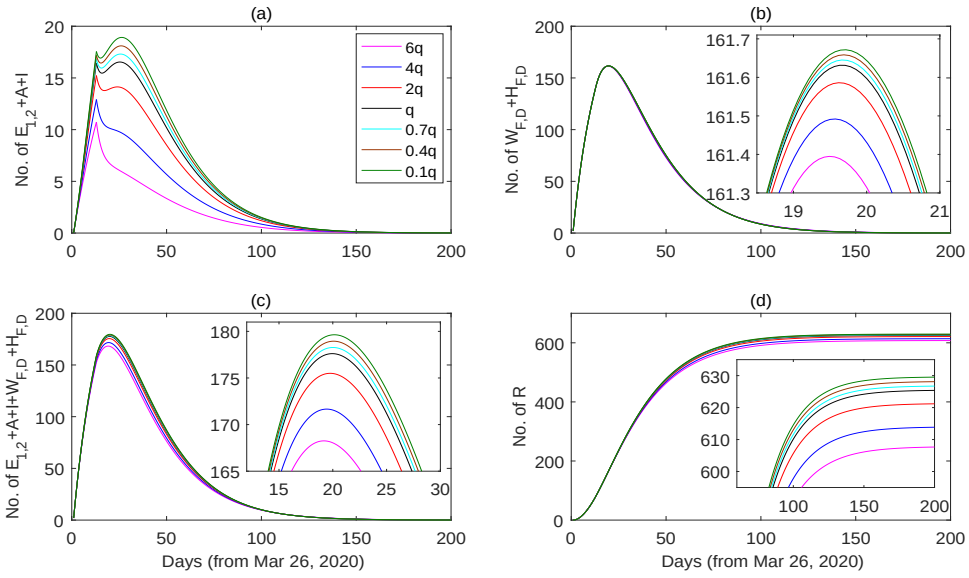

Figure S1. The effects of varying quarantine rate q on the early control of COVID-19 epidemic in Heilongjiang Province, China. The baseline parameter values and initial values are the same as in Tables 1, 2 and 3.

From Figure S1, compared with the baseline situation, when the quarantine rate is strengthened or weakened, the second index will hardly changes, while the first, third and fourth indexes will decrease

or increase slightly, respectively. Especially, when the quarantine rate is greatly strengthen even by 6 times, there are also relative small or slightly changes on the last three indexes, and there is larger changes on the first index. Specifically, the peak or stable states for the last three indexes are only reduced by about 66.20%, 0.19%, 5.49% and 2.8%, respectively. It means that the change of quarantine rate mainly impact the potential transmission risk and the final size of the disease, and the actually intensive contact tracing and quarantine are effective in the early border control stage.

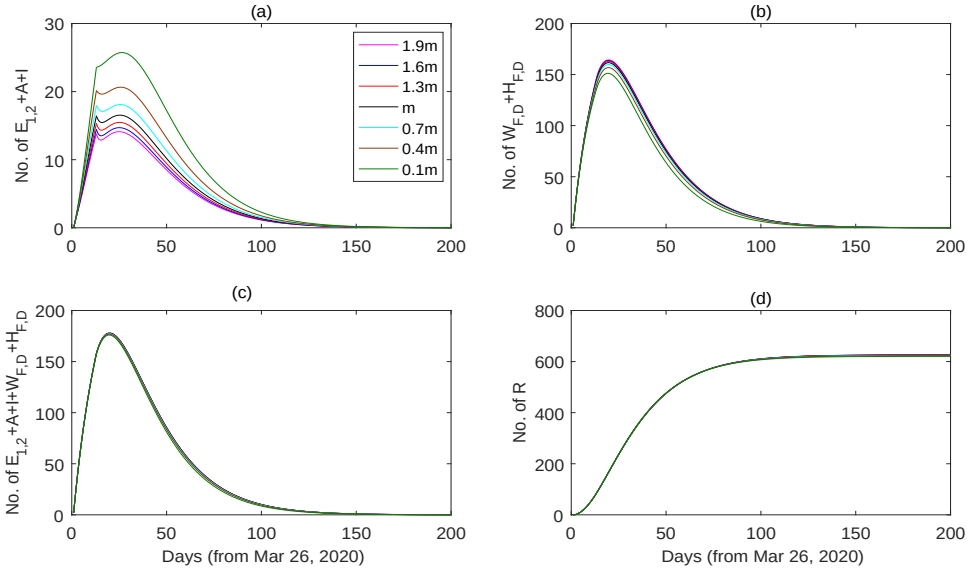

Figure S2. The effects of varying test rates m_{E_2}, m_A and m_I on the early control of COVID-19 epidemic in Heilongjiang Province, China. Here m denotes $m_i (i = E_2, A, I)$. The baseline parameter values and initial values are the same as in Figure S1.

It follows from Figure S2 that with the increase of testing rates, the first two indexes will slightly decrease and increase, respectively. There is almost no change on the last two indexes due to the balance of the two opposite effects. Moreover, when the testing rate is weakened from the baseline value, there are relative small changes on the first index. However, when the testing rate is strengthen from the baseline value, there are larger changes on the first two indexes, especially for their peak values. It means that the change of testing rate mainly impacts the potential transmission risk and the treatment situation, that the actually testing intensities are effective in the early stage, and that the potential transmission risk will worsen once the testing intensity is relaxed.

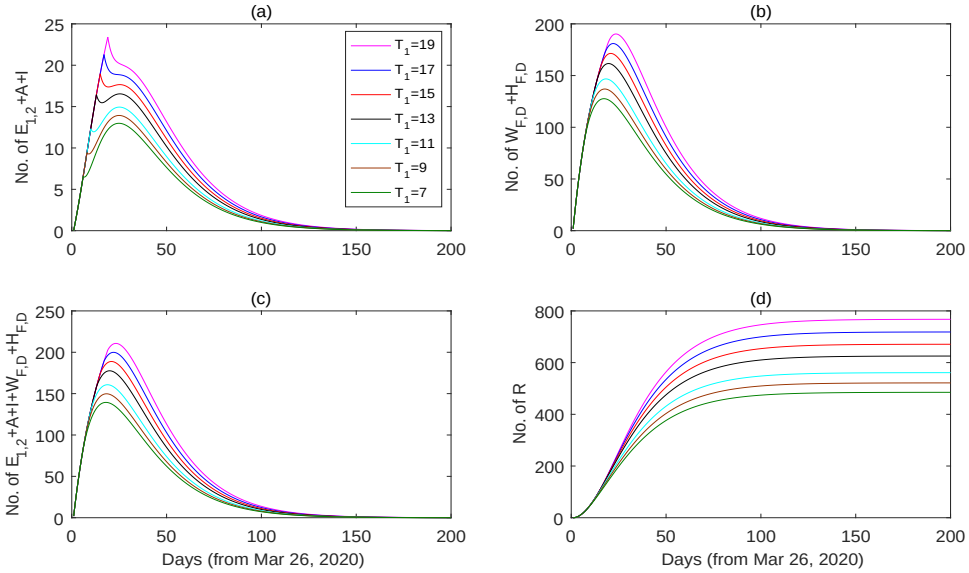

Figure S3. The effects of varying the border closure time T_1 on the early control of COVID-19 epidemic in Heilongjiang Province, China. The baseline parameter values and initial values are the same as in Figure S1.

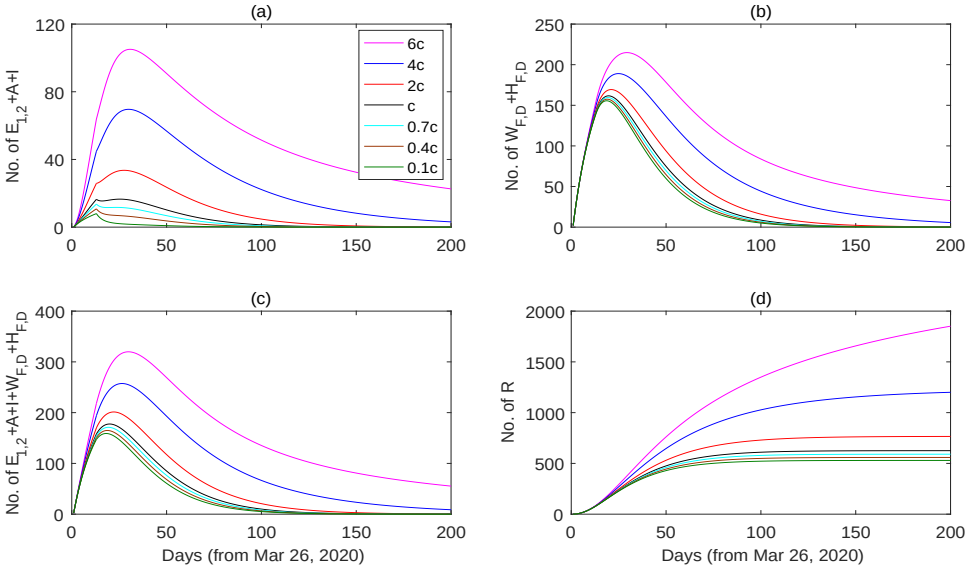

Figure S4. The effects of varying the contact rate c on the early control of COVID-19 epidemic in Heilongjiang Province, China. The baseline parameter values and initial values are the same as in Figure S1.

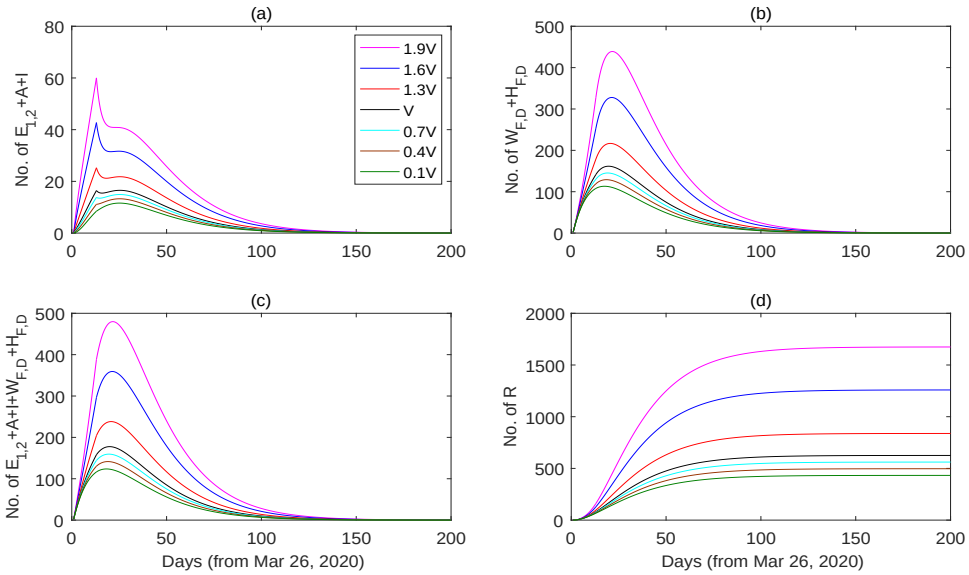

Figure S5. The effects of varying the quantities of illegal and legal importing population $V_i(t)(i = p, q)$ on the early control of COVID-19 epidemic in Heilongjiang Province, China. Here V denotes $V_i(t)(i = p, q)$. The baseline parameter values and initial values are the same as in Figure S1.

From Figures S3, S4 and S5, the four indexes will decrease by reducing the border closure time T_1, contract rate c or the quantity of importing individuals $V_i(t)(i = p, q)$. Compared with the baseline situation, the four indexes are stably decreased (or raised) by reducing (or increasing) T_1 or c, and they are sharply decrease (or raised) with by reducing (or increasing) $V_i(t)(i = p, q)$. It indicates that the changes of the border closure time, contact rate and the quantity of importing individuals will greatly impact the four indexes, that the those actual control intensities are effective in the early stage, and that the four indexes will worsen once the actual border closure time is delayed or the actual contact rate and the quantity of importing individuals are increased.

In summary, it follows from Figures S1, S2, S3, S4 and S5 that the actual border control intensities in Heilongjiang Province are relative effective in the early border control stage, and the rebound of COVID-19 epidemic will be worsen once the actual border control strategies are relaxed.